ARTICLE IN PRESS

International Journal of Plasticity xxx (2010) xxx–xxx

Contents lists available at ScienceDirect

International Journal of Plasticity

journal homepage: www.elsevier.com/locate/ijplas

The role of grain boundaries on fatigue crack initiation – An energy approach

Michael D. Sangid [a], Hans J. Maier [b], Huseyin Sehitoglu [a,*]

[a] Department of Mechanical Science and Engineering, University of Illinois at Urbana-Champaign, 1206 W. Green St., Urbana, IL 61801, USA
[b] Lehrstuhl für Werkstoffkunde (Materials Science), University of Paderborn, 33095 Paderborn, Germany

ARTICLE INFO

Article history:
Received 6 August 2010
Received in final revised form 14 September 2010
Available online xxxx

Keywords:
Fatigue
Grain boundaries
Polycrystalline material
Energy methods
Persistent slip bands

ABSTRACT

In this paper, we construct a model for prediction of fatigue crack initiation based on the material's microstructure. In order to do so, the energy of a persistent slip band (PSB) is monitored and an energy balance approach is taken, in which cracks initiate and the material fails due to stress concentration from a PSB (with respect to dislocation motion). These PSBs are able to traverse low-angle grain boundaries (GB), thus belonging to clusters of grains. As a consequence of the ongoing cyclic slip process, the PSBs evolve and interact with high-angle GBs, the result of which leads to dislocation pile-ups, static extrusions in the form of ledges/steps at the GB, stress concentration, and ultimately crack initiation. Hence, this fatigue model is driven by the microstructure, i.e. grain orientations, widely distributed grain sizes, precipitates, PSB–GB interactions, as well as the affect of neighboring grains. The results predict that cracks initiate near twin boundaries from PSBs spanning a single large grain with a favorable orientation or multiple grains connected by low-angle GBs. Excellent agreement is shown between model predictions and experimental data.

1. Introduction

1.1. PSB–GB interactions

Fatigue crack initiation in pure FCC metals is most commonly a result of persistent slip bands (PSBs) at mid-to-low strain amplitudes (Differt et al., 1986; Essmann et al., 1981; Essmann and Mughrabi, 1979). Initial studies of the PSB mechanisms focused on copper single crystals, although similar dislocation arrangements have been observed in polycrystalline material (Buque, 2001; Buque et al., 2001a, 2001b; Li et al., 2008). In these materials, PSBs form in large grains with high Schmid factors (Blochwitz et al., 1996; Miao et al., 2009; Weidner et al., 2006).

Over the years, several models have emerged to explain PSB mechanisms in polycrystalline material and their role in crack initiation. The dislocation arrangements in polycrystals are similar to those in single crystals, except that the dislocations are impeded by the grain boundary (GB) resulting in pile-up and stress concentration (Essmann et al., 1981). The resulting stress is relieved by formation of a static extrusion at the GB; expressions are formulated for the resulting slip and static extrusion height at the GB (Mughrabi et al., 1983). Over an increasing number of cycles, the stress concentration and extrusion height increases assisting in crack nucleation at the PSB–GB interface. Crack initiation may occur away from GBs, although this is typically seen in materials with defects, inhomogeneities, or very large (average) grain sizes. In superalloy technology, processing improvements have led to a significant reduction of defects within this material reducing this mode of failure; hence this study focuses on PSB–GB driven failures.

* Corresponding author. Tel.: +1 217 333 4112.
E-mail address: huseyin@illinois.edu (H. Sehitoglu).

0749-6419/$ - see front matter © 2010 Elsevier Ltd. All rights reserved.
doi:10.1016/j.ijplas.2010.09.009

Please cite this article in press as: Sangid, M.D., et al. The role of grain boundaries on fatigue crack initiation – An energy approach. Int. J. Plasticity (2010), doi:10.1016/j.ijplas.2010.09.009

Lin and Ito developed a model for plastic shear strain accumulation from a PSB in a polycrystal (Lin and Ito, 1969). Building on their concepts, Tanaka and Mura created an energy balance of the dislocation arrangement along the PSB, in order to predict crack initiation (Tanaka and Mura, 1981). Both of these models develop a strong foundation for modeling PSB behavior in polycrystals, although they assume an extremely simply dislocation arrangement within the PSB and do not account for PSB–GB interactions, which is a precursor to crack initiation. In this study, we create an energy approach to model PSB behavior in a polycrystal based on PSB–GB interactions.

GBs have been described as impenetrable obstacles to PSBs that cause stress concentration resulting in cracking or PSB formation in adjacent grains (Dorr and Blochwitz, 1987). Since that time, the misorientation and Schmid factor of adjacent grains have been recognized as important parameters in determining PSB–GB interaction and crack initiation (Blochwitz et al., 1995). Based on experimental observation by Zhang et al. PSBs can transmit through low-angle GBs (LAGBs), hence cracking does not occur in these boundaries (Kobayashi et al., 2009; Zhang and Wang, 2003; Zhang et al., 1998). LAGBs are defined as a misorientation between grains of less than 15° (Appendix A), also referred to, in literature, as a $\Sigma 1$ GB according to the coincident site lattice (CSL) (Grimmer et al., 1974; Kronberg and Wilson, 1949) theory using the Brandon condition (Brandon, 1966). Interestingly, PSBs cannot transfer through general (random) high-angle GBs (HAGBs), resulting in impedance of dislocation motion, dislocation pile-ups, stress concentration, and intergranular fracture (Zhang and Wang, 2000a). Further, the mechanism of HAGB cracking is independent of the angle between the applied stress axis and the GB plane (Zhang et al., 2003). From this analysis, the PSB–GB interaction can result in dislocations behaving by one of the following scenarios: passing through, piling-up, or partially passing through (resulting in a residual dislocation within the GB) (Zhang and Wang, 2000b, 2000c). For the latter case, the GB orientation and character plays an important role (Wang et al., 2001). The GB character can be quantified by the CSL notation, as an outcome special CSL boundaries do not experience intergranular cracking (Kobayashi et al., 2008; Lim, 1987), especially the $\Sigma 3$ boundaries also known as twins, which are discussed later in this section. These experimental observations are leveraged in our model to predict fatigue crack initiation via PSBs.

The stress necessary to cause cracking at a PSB–GB interface was first calculated by Essmann et al. (1981), in which the slip vector is directly related to the grain diameter. This analytical expression for stress was amended by Christ (1989) and Liu et al. (1992) to include the number of dislocations within the pile-up (Eshelby et al., 1951) and the angle between the pile-up and GB (Stroh, 1957). Their analyses showed that coarser grains and high energy GBs were preferred sites for cracking, although their models over predicted the shear stress necessary for crack initiation. Based on the assumption that the PSB forms over a quarter of the grain diameter, the concept was extended to provide more accurate theoretical stresses (Burmeister and Richter, 1997). The amount of slip that penetrates the GB was calculated, which reduces rapidly with increasing misorientation (Lin et al., 1998). Each of these models provide a valuable contribution to the field, although they cannot predict failure, since most of the variables in their analysis do not evolve with increasing loading cycles, nor do they account for the effect of neighboring grains as is the focus in our model.

1.2. The role of TBs in fatigue

Experimentally, twin boundaries (TBs) have been observed as preferred sites for crack initiation (Hashimoto et al., 1999; Llanes and Laird, 1992; Miao et al., 2009), although there is still debate on the TB's fatigue response in FCC material. In other words, do TBs harden the material or degrade the fatigue life by acting as crack nucleation sites? Initially, Bottner, McEvily, Liu observed the formation of fatigue cracks at TBs (Boettner et al., 1964). In many cases, the PSBs form parallel to the TB's normal, resulting in PSB–TB interaction. They note coherent TBs as low energy interfaces within the material, but as PSBs intersect the TBs, non-coherent ledges, steps, or static extrusions form on the TBs. The resulting steps are non-coherent, facilitators of secondary slip, dislocation sources, stress concentrators, and preferred crack initiation sites, as shown in Fig. 1a–c. The same phenomenon was observed by Thompson (1972). He concluded larger grains and lower stacking fault energies (SFE) result in greater dislocation pile-ups (Fig. 1d) and more secondary slip, respectively; as a consequence both factors result in more stress concentration and are more prone to cracking. In other words, TBs are inherently stronger against intergranular cracking in materials with high SFE, while in low SFE materials, TBs accommodate much of the plastic deformation leading to stress concentration and crack nucleation at the TB (Qu et al., 2008). Interestingly, in nanocrystalline material, thinner twins (<1 μm) play an important role in strengthening the fatigue response of the material by affecting the type of PSB–TB interaction (Guo et al., 2005).

Many models are available to explain TBs as preferred sites for crack nucleation (Blochwitz et al., 1995). Kim and Laird argued that plastic incompatibilities caused by surface steps at the TB lead to irreversibilities (Fig. 1e) and cracking (Kim and Laird, 1978). Lim and Raj presented a dislocation model as shown in Fig. 1f, in which they measured the residual or sessile dislocations at the boundary and from this quantity coined a continuity factor dependent on the slip transfer (Lim and Raj, 1985). Neumann created a traction model to calculate the local stress concentration at TBs promoting crack initiation at low plastic strain amplitudes (HCF), as shown in Fig. 1g (Heinz and Neumann, 1990). Peralta et al. modeled the elastic incompatibilities near a TB (Fig. 1h); from this analysis, they calculated the stress concentration, which is a maximum value when the tensile axis is a ⟨1 1 1⟩ direction, i.e. the loading axis is parallel to the TB (Peralta et al., 1994). In this model, the TBs promote early primary slip and secondary slip. Peralta's elastic incompatibility results were reconstructed using the finite element method (Lewis et al., 2008; Sumigawa and Kitamura, 2004); the results are in agreement and show that coherent TBs have the highest elastic stress concentrations. Building on these concepts, Neumann's model was modified by Blochwitz and Tirschler to account for medium plastic strain amplitudes, thus representing an elasto-plastic solution, as shown in Fig. 1i

Please cite this article in press as: Sangid, M.D., et al. The role of grain boundaries on fatigue crack initiation – An energy approach. Int. J. Plasticity (2010), doi:10.1016/j.ijplas.2010.09.009

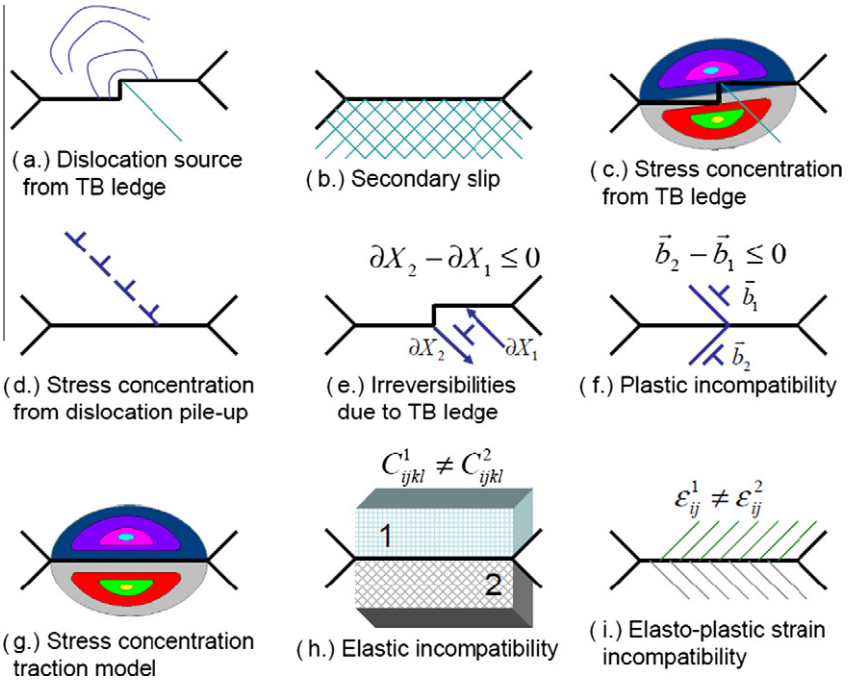

Fig. 1. Theories describing crack initiation at twin boundaries (TBs). (a) Ledges/steps at the TB are noncoherant and effective sources for dislocation nucleation (Boettner et al., 1964). (b) Due to the stress concentration at the TB, secondary slip is activated (Boettner et al., 1964); which is more prevalent in low SFE materials (Thompson, 1972). (c) Ledges/steps result in stress concentration (Boettner et al., 1964). (d) Dislocations pile-up at the TBs resulting in stress concentration, which is more dominant in larger grains (Thompson, 1972). (e) Ledges/steps at the TB results in irreversible slip (Kim and Laird, 1978). (f) Plastic incompatibility as a result of incoming and outgoing glissile dislocations interaction with the GB (Lim and Raj, 1985). (g) Stress concentration is due to traction at the surface and TBs (Heinz and Neumann, 1990). (h) Elastic incompatibility is highest at the TB (Peralta et al., 1994). (i) Extension of (h) to include plastic strain incompatibility (Blochwitz and Tirschler, 2003, 2005).

(Blochwitz and Tirschler, 2003, 2005). Each of the aforementioned models demonstrates the role of TBs as preferred sites for fatigue crack initiation in polycrystalline material.

These experimental results and analytical models provide a solid foundation for our model, which overwhelmingly illustrate that cracks preferentially nucleate near TBs as a consequence of dislocation pile-up and stress concentration. This is illustrated through atomistic-based calculation of the energy barrier for slip-GB interaction in this paper, in which TBs have the largest value. Also, in our analysis, we describe an approach to model the energy of a PSB structure and use its stability with respect to dislocation motion as our failure criterion for fatigue crack initiation. From this analysis, we are able to predict the fatigue life of polycrystalline specimens, which rely heavily on PSB–GB interactions. It is our purpose to rationalize the long standing observation of the role of TBs in fatigue with modeling at the atomic and continuum scales, thus we provide a unified framework for clear understanding of TBs.

2. Material and experimental methods

In this study, we formulate a model for predicting fatigue crack initiation in a wrought Ni-based superalloy, Udimet 720 (U720), although this methodology could be used to characterize fatigue in a variety of metals and alloys. This material was chosen due to the complexities and wide-distributions of microstructural features (especially grain size variability), further validating our model. The material exhibits a large twin volume fraction (low stacking fault energy), is susceptible to the formation of persistent slip bands through shearing the matrix and precipitates, and at the same time, is interesting from an application point of view.

The primary strengthening mechanism in this material is in the form of ordered Ni_3Al precipitates ($L1_2$ structure), which occur in this material at three length scales (primary, secondary, and tertiary). The coherency of these γ' precipitate with respect to the γ matrix offers stability along with enhanced strengthening at elevated temperatures. The material underwent a solution process at 1100 °C for 2 h followed by oil quenching, in order to prepare the matrix for uniform precipitation of γ'. Afterwards, it was aged at 760 °C for 8 h with air-cooling, in order to precipitate the coarser γ', which offers creep resistance. A second aging process at 650 °C for 24 h with air-cooling produced fine γ' thus strengthening the microstructure for tensile and fatigue loads and stabilizing the γ' precipitates.

Also, during the heat treatment process the γ' acts to pin the grain boundaries, thus determining the grain size in the γ matrix. In this material, there are areas of densely populated γ' along side areas denuded of γ'. As a result, there exists a wide

Please cite this article in press as: Sangid, M.D., et al. The role of grain boundaries on fatigue crack initiation – An energy approach. Int. J. Plasticity (2010), doi:10.1016/j.ijplas.2010.09.009

distribution of grain sizes, as fine grains form in regions of heavily populated γ' and coarse grains form in regions where γ' is sparse. Data on grain size and orientation was obtained from EBSD scans on three samples: (1) fatigue specimen tested at the highest strain range, (2) fatigue specimen tested at the lowest strain range, and (3) an as-received specimen. From these results, we see that fatigue testing did not significantly affect the texture of the material. The individual statistics of the three specimen's microstructure are shown in Table 1. By pooling all three EBSD scans in to one population, we can develop a representative characterization of the U720 microstructure. The mean grain size is 3.4 μm although the grain size distribution has a large tail indicating many larger grains are present (Fig. 2a). Further, due to the variation in grain sizes and neighboring grains, each grain can have a wide distribution of associated GBs. From this analysis, the CSL value of each GB is determined by the methodology described in Appendix A and shown in Fig. 2b.

In this study, strain-controlled low cycle fatigue experiments were conducted on U720 specimens at three total strain ranges (we refer to normalized values of 1.00%, 0.73%, and 0.69%, whereas each strain range is divided by the maximum tested strain range) at elevated temperature and $R_\varepsilon = 0$. The resulting hysteresis response displays considerable material compression during unloading and minimal ratcheting. Crack initiation was defined as the measured load dropping to a level of 90% of the saturated value. The fracture surface of the failed fatigue specimens were analyzed to study the mechanism for crack initiation, as shown in Fig. 3a and b. From Fig. 3a and b, twinning is observed near the facet features, thus indicating that cracks initiate near the TBs, as reported in literature (Boettner et al., 1964; Guo et al., 2005; Hashimoto et al., 1999; Llanes and Laird, 1992; Miao et al., 2009; Qu et al., 2008; Thompson, 1972). A histogram of the size of these facet features is shown in Fig. 2c representing 89 fatigue experiments.

Material characterization in the form of TEM was performed, which provided a qualitative indication of the material behavior, thus providing key insights that can be used to model the microstructure and resulting dislocation arrangements. In the fatigued samples, slip and plastic strain are localized into banded regions. Fig. 3c shows a low-magnification TEM image of persistent slip bands in U720, and a more detailed view of two bands in this structure is shown in Fig. 3d. From this TEM analysis, we draw many insights into the strain localization that ultimately leads to failure within U720. Slip interacts with the grain boundary causing pile-up of dislocations and stress concentration, which results in slip transmission into the second grain. By viewing the high magnification image, we see that the slip band forms by dislocations shearing the γ' precipitates resulting in slip being confined to a single glide plane (a 2D planar feature).

3. Energy approach and balance

The aim of this model is to predict failure for polycrystals which exhibit PSBs, in these materials the PSB–GB interaction governs the fatigue life. Our approach is to model the energy of a persistent slip band structure, E, and use its stability with respect to dislocation motion as our failure criterion for fatigue crack initiation. This approach allows us to address the small-length scale problems via incorporation of atomistic simulations. Hence, the atomistic simulations provide important insights into the energy barriers and physics of the grain boundaries, which are crucial to fatigue of a polycrystalline material. All the contributing energy factors to the PSB are addressed and our energy balance is as follows:

$$E = -E^{\sigma}_{app}(\sigma, m, L, N) - E_{hard}(\rho, L, N) + E^{disl}_{pile\text{-}up}(h, d, L, N) + E^{disl}_{nuc}(m, \Sigma, h, L, L', N) + E^{PSB-GB}_{interaction}(m, \Sigma, h, L, L', N) + E^{PSB-GB}_{LAGB}(m, \Sigma, h, L, L', N) + E_{APB}(L, \gamma'_{dist}, N) + E_{\gamma\text{-}SF}(L, \gamma'_{dist}, N) \quad (1)$$

where σ is the applied stress during fatigue loading, N is the number of cycles, m is the Schmid factor of the grain containing the PSB, L is the grain size, L' is the grain size of the neighboring grain, h is the height of the PSB, d is the mean dislocation spacing within the PSB, ρ is the dislocation density within the PSB, Σ is the character of GB in the CSL, and γ' is the distribution of Ni_3Al precipitates in terms of volume/area fraction (Sangid et al., in press-a). Eq. (1) can be interpreted as the balance of external mechanical work in terms of driving the dislocations to the stored mechanical potential energy related to elastic and defect/fault energies. The first three terms of the energy expression displays terms that are associated with the continuum mechanics concepts for modeling dislocations in otherwise homogeneous media, and the other terms are derived by atomistic simulations. Each term is discussed in the subsequent sections.

Table 1
Statistics of EBSD characterization on the specimen's microstructure.

	Specimen 1	Specimen 2	Specimen 3
Number of grains	2373	3664	7424
Average grain size (μm)	5.3	4.2	2.4
Grain size standard deviation (μm)	2.2	1.9	0.9
Largest grain size (μm)	18.4	16.7	8.3
Average # of GBs per 2D grain scan	5.6	5.6	5.4
Average Schmid factor	0.450	0.451	0.456
Low angle GB (LAGB or Σ1) fraction	13.2%	17.4%	9.4%
Σ3-twin boundary fraction	48.3%	46.9%	46.3%
Taylor factor of aggregate	3.065	3.074	3.071

Please cite this article in press as: Sangid, M.D., et al. The role of grain boundaries on fatigue crack initiation – An energy approach. Int. J. Plasticity (2010), doi:10.1016/j.ijplas.2010.09.009

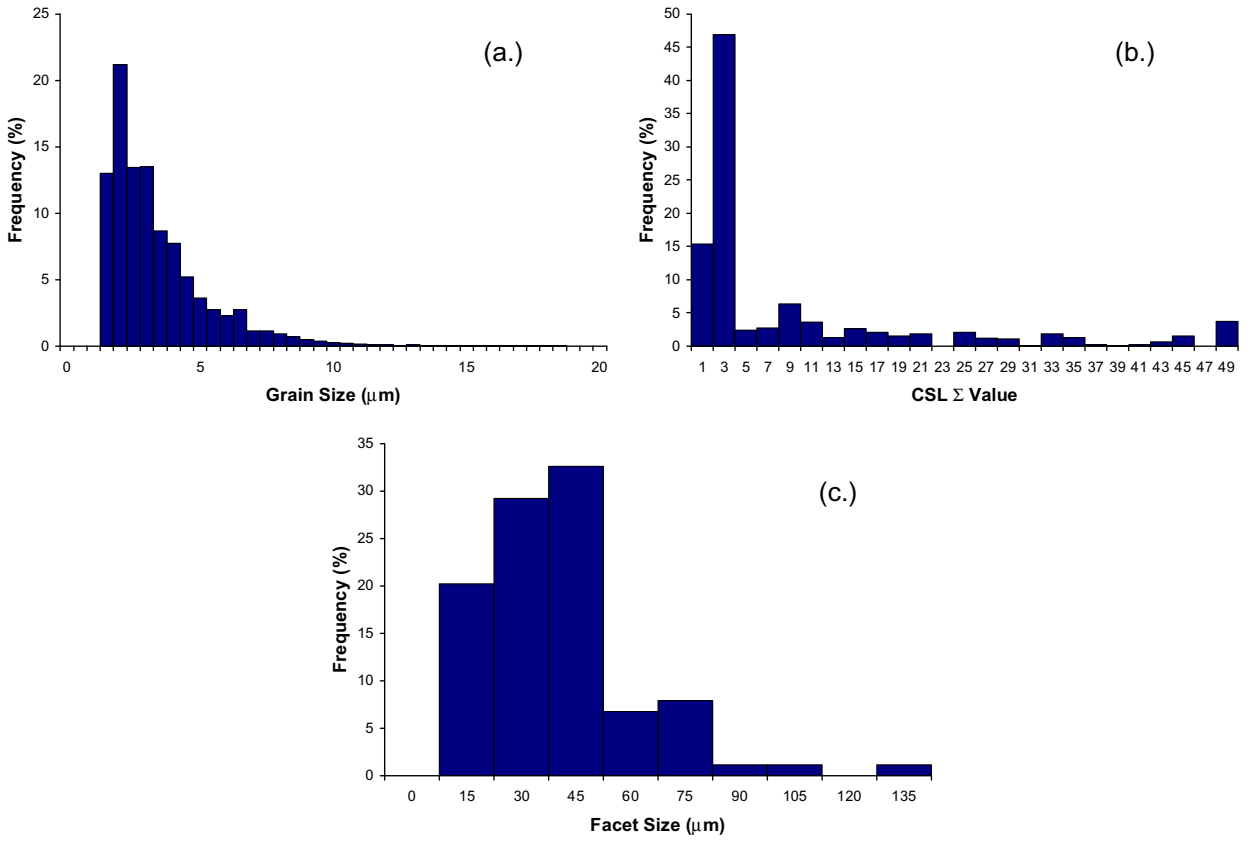

Fig. 2. By pooling the EBSD results from three specimens (Table 1), histograms are calculated of the (a) grain size and (b) GB character in terms of the CSL Σ values. (c) A histogram of the facet size measured from SEM of the failed experimental fatigue specimens, corresponding with Fig. 2a and b.

The geometry of the PSB within the most favorably oriented grain of a polycrystal is shown in Fig. 4; from which, it can be seen that the dislocations localize into the PSB. The PSB intersects the GB, as a consequence of slip within the PSB. Further, the interactions between PSBs and GBs in polycrystals results in the formation of a static extrusion or ledges/steps, thus roughening the GB.

3.1. Continuum stress field terms

The continuum terms (first three terms in Eq. (1) create an internal stress field, E_τ; the glissile dislocations must overcome this stress field to plastically deform the material (Eshelby et al., 1951) by an increment of slip, ∂X_i, as follows:

$$E_\tau = -E^{\sigma}_{app} = E_{hard} + E^{disl}_{pile\text{-}up} + E^{disl}_{nuc} = \sum_i \bar{\tau}\vec{b}Ln^{layers}\partial X_i \tag{2}$$

where the overall shear stress, $\bar{\tau}$, is composed of the contribution from the dislocation field in the PSB structure, τ^{dis}, the work-hardening of the system, τ^h, and the external applied resolved shear stress, τ^A.

$$\bar{\tau} = \tau^{dis} - \tau^h - \tau^A \tag{3}$$

The concepts of superposition of the stress fields (including external applied stresses and dislocation–dislocation interactions) on the movement of dislocations have a long standing foundation in continuum mechanics modeling (Sofronis and Birnbaum, 1995). Each of these terms are modeled at the elevated fatigue test temperature, therefore this formulation is valid at these elevated isothermal conditions. It is paramount to account for each layer of successive dislocations that are gliding within the PSB. The number of moving planes within the PSB is quantified by n^{layers}, which is related to the PSB width, h.

$$n^{layers} = h/y^e \tag{4}$$

The width of the PSB, h, was measured from the TEM images of U720 (e.g. Fig. 3d). This quantity was seen to increase according to a square root function with increasing number of cycles and saturate. The width of the PSB must be normalized by the distance between dislocations within the PSB to find the number of layers; in order to do so, the annihilation distance,

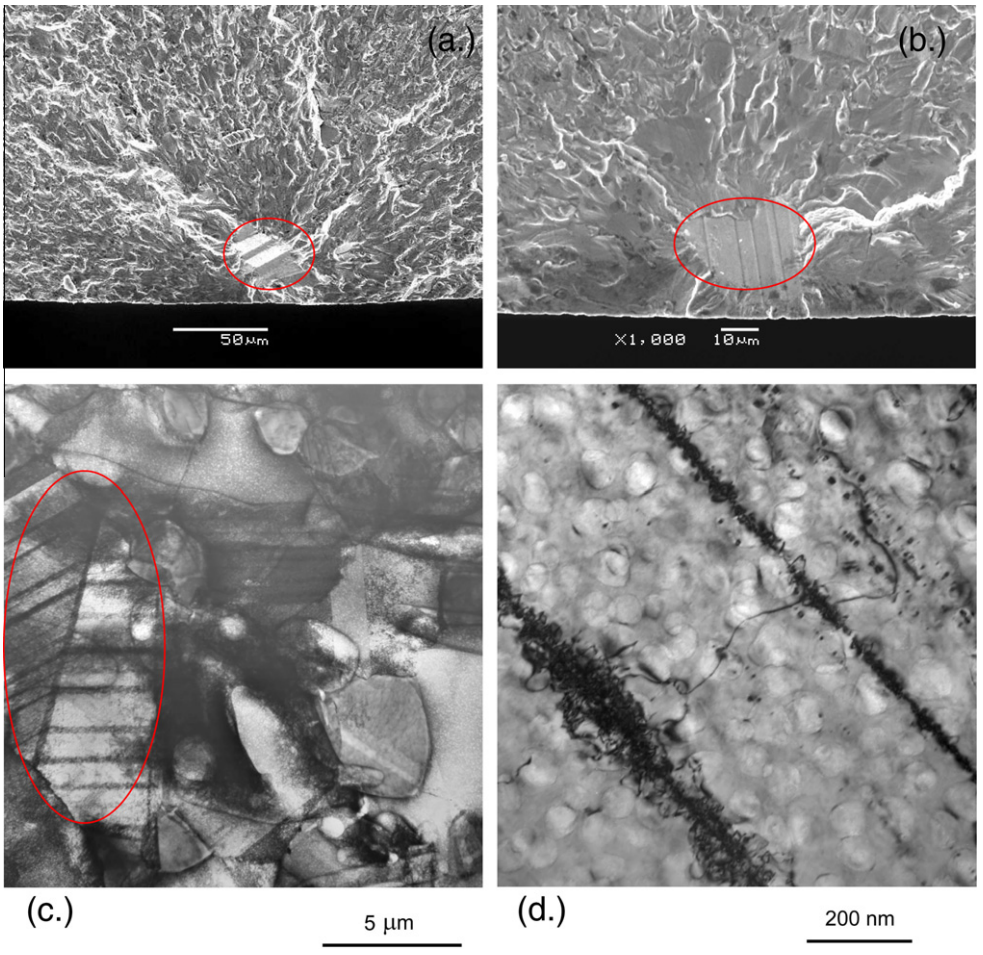

Fig. 3. (a and b) Fracture surface of a failed fatigue specimen, cracks initiate from facets, although considerable plasticity is involved in forming this feature. From the pictures, we can see evidence of twinning near the facets (c). A low-magnification TEM image of a persistent slip band (shown within the red ellipse). (d) A high-magnification image of two bands in a failed fatigue specimen of U720 tested at a high strain range, $R = 0$, and 538 °C. (For interpretation of the references to colour in this figure legend, the reader is referred to the web version of this article.)

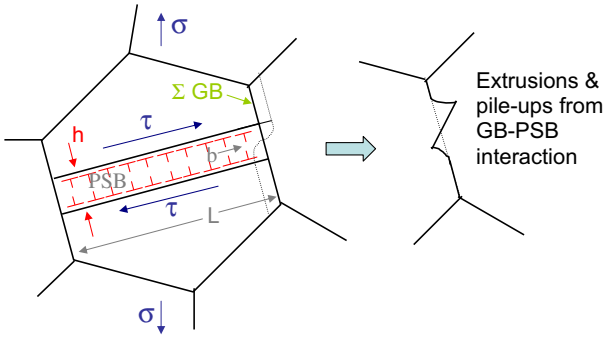

Fig. 4. Schematic of the PSB geometry in the polycrystal. The PSB forms across a grain of size L and a given orientation (Schmid factor, m) and intersects a pair of GBs each with an associated Σ value. The PSB interaction with GBs leads to static extrusions across the GB in the form of ledges and steps.

y^e, of edge dislocations within a PSB is used. This quantity was originally calculated by Essmann and Mughrabi (1979), who theorized that during saturation of the PSB, the dislocations approach this annihilation distance. The individual stress components that contribute to the internal stress field are discussed next.

Please cite this article in press as: Sangid, M.D., et al. The role of grain boundaries on fatigue crack initiation – An energy approach. Int. J. Plasticity (2010), doi:10.1016/j.ijplas.2010.09.009

3.1.1. Dislocation pile-up

Within the PSB, dislocations agglomerate and form dipole structures, in order to minimize their total energy, as discussed by Kuhlmann-Wilsdorf (1989), Kuhlmann-Wilsdorf and Laird (1977) and observed experimentally for a Ni-based superalloy (Huang et al., 2010). These dislocation arrangements have historically been modeled as layers of opposing signed dislocations (Essmann et al., 1981; Tanaka and Mura, 1981) separated by a distance, h. Within each layer is a series of dislocations, equally spaced by d. Recently, more advanced modeling techniques have been used to address this type of dislocation arrangement. Van der Giessen and Needleman developed a dislocation dynamics model to verify that the stress field from a series of planar edge dislocations can be modeled as a series of hyperbolic terms (van der Giessen and Needleman, 1995). Brinckmann extended this model to account for two opposing series of edge dislocations, which provided a good approximation for the dislocation arrangement in a PSB and the resulting stress field (Brinckmann, 2005).

Our model does indeed assume a simplified version of the dislocation arrangement, although it is consistent with past researchers in terms of experimental observations (Huang et al., 2010), which were modeled using dislocation dynamics to obtain analytical solutions (Brinckmann, 2005; van der Giessen and Needleman, 1995). In doing so, we can assume linear elastic, isotropic, plane strain behavior thus greatly simplifying the problem, in order to find the stress within the PSB. The stress field created by the dislocation dipoles within the PSB is given by τ^{dis} as it varies spatially (x, y) within the PSB (Brinckmann, 2005):

$$\tau^{dis} = \frac{\mu b \pi}{(1-\nu)d^2}\left(\frac{y\left(1-\cos\left(\frac{2\pi x}{d}\right)\cosh\left(\frac{2\pi y}{d}\right)\right)}{\left(-\cos\left(\frac{2\pi x}{d}\right)+\cosh\left(\frac{2\pi y}{d}\right)\right)^2}-\frac{(h+y)\left(1-\cos\left(\frac{2\pi x}{d}\right)\cosh\left(\frac{2\pi(h+y)}{d}\right)\right)}{\left(-\cos\left(\frac{2\pi x}{d}\right)+\cosh\left(\frac{2\pi(h+y)}{d}\right)\right)^2}\right) \tag{5}$$

where the elastic constants μ, ν are the shear modulus and Poisson ratio at elevated temperatures, respectively. The mean dislocation spacing, d, is determined based on the dislocation density within the PSB, ρ, as follows:

$$d = \frac{1}{\sqrt{\rho}} \tag{6}$$

The resulting energy produced by the patterned dislocation structure in our model is similar to the formulization present by Biermann et al. (1993), Huang et al. (2010), Kuhlmann-Wilsdorf (1989), although the logarithmic cutoff radius in their solution is replaced with a more accurate series of hyperbolic terms established from dislocation dynamics modeling to address long-range stresses (Brinckmann, 2005; van der Giessen and Needleman, 1995). It is suggested by Huang et al. (2010) that the evolution of dislocation substructures represented in this section results in irreversible strain and fatigue damage.

3.1.2. Work-hardening

As previously mentioned dislocations shear a given precipitate and weaken the effective area of the particle, which makes it easier for subsequent dislocations to cut the particle on the same slip plane. The dislocations accumulate and interact with each other, resulting in significant work-hardening within the PSB (Essmann and Mughrabi, 1979; Friedel, 1957; Grosskreutz, 1971; Huang et al., 2008; Seeger et al., 1957). This work-hardening in many ways can relax the elastic stored energy during cyclic loading. Hence, it must be taken into account. In this model, the work-hardening of dislocations within the PSB is assumed to follow a Taylor relationship (Mughrabi, 1983):

$$\tau^h = \alpha \mu b \sqrt{\rho} + \tau_o \tag{7}$$

where the scalar, $\alpha = 0.45$ (Argon, 2008). The initial shear stress, τ_o:

$$\tau_o = \frac{\sigma_y}{M} \tag{8}$$

is given by the yield stress at the test temperature normalized by the Taylor factor, M, which is random ($\sim$3.06) for this material. The evolution of dislocation density with loading cycles (N) was extracted from literature for a similar Ni-based superalloy studied by Huang et al. (2008). Since Huang's study only represents one test condition, the functional form of the dislocation density was amended according to Appendix B.

3.1.3. Applied stress

The applied shear stress for each grain, τ^A, is calculated from the hysteresis behavior of the material during the strain control test, i.e. the stress range is multiplied by the Schmid factor of the individual grain, m.

$$\tau^A = m \cdot \Delta\sigma^A = m \cdot H(N) \tag{9}$$

The evolution of alternating stress during loading, $\Delta\sigma^A$, is obtained from the macroscopic response of the test data for the polycrystalline material, U720. The stress response, $H(N)$, resembles a square root function as it hardens with increasing number of cycles and saturates. The stress is dependent on the applied strain, although at each strain range, the stress saturates after approximately 100 cycles; similar behavior for Ni-based superalloys were observed by Huang et al. (2010).

In this model, the contributions of stress from the dislocation pile-up, work-hardening, and applied stress are superimposed into a stress field, which glissile dislocations within the PSB must overcome to plastically deform the material. In Eq.

Please cite this article in press as: Sangid, M.D., et al. The role of grain boundaries on fatigue crack initiation – An energy approach. Int. J. Plasticity (2010), doi:10.1016/j.ijplas.2010.09.009

(1), the first three terms represent the contribution in stress field from each of these components; the sum of these stress fields represents the internal stress field energy in the PSB, which we use continuum mechanics concepts for modeling dislocations in otherwise homogeneous media.

3.2. Atomistic contributions

During the fatigue process, dislocations nucleate and shear the γ' precipitates to form slip bands. Once formed, the dislocations within the PSB interact with the GB. In order to capture the physics at the grain boundary interface, it is necessary to investigate this problem at a smaller scale. Hence, atomistic simulations in the form of molecular dynamics (MD) are utilized and the results are incorporated into the energy balance in the form of energy barriers to slip. It should be noted that these terms are not purely MD-based; they combine MD results with certain volume averaging concepts, geometry, and continuum ideas. As previously mentioned, the GBs within the microstructure of U720 were characterized by EBSD and the corresponding energies were measured from MD Sangid et al. (2010), as shown in Fig. 5a. The following addresses the last five terms in Eq. (1).

3.2.1. Dislocation nucleation from GB and agglomerating in the PSB

Dislocations nucleate during fatigue loading and agglomerate in the PSB resulting in a hardening response. GBs act as distinct sources for dislocations. Depending on the character of each GB, there is a different energy barrier for dislocation nucleation. In Appendix C, it was have shown that the energy barrier for nucleation, $E_{MD}^{\gamma\text{-}nuc\text{-}GB}$, is inversely related to the static GB energy, E_{Static}^{GB}, through a power law relation (Fig. 5b):

$$E_{MD}^{\gamma\text{-}nuc\text{-}GB} = 6.0 \times 10^{15} \cdot \left(E_{Static}^{GB}\right)^{-1.3} \tag{10}$$

Hence, GBs with stable configurations and low interface energy have a larger energy barrier to nucleate a dislocation. With this information, we can model the energy associated with the nucleation of dislocations from a distinct GB as:

$$E_{nuc}^{disl} = \sum\nolimits_i \partial X_i \cdot E_{MD}^{\gamma\text{-}nuc\text{-}GB}(\rho - \rho_o)\vec{b}hL^2 \tag{11}$$

The number of dislocations nucleating within the PSB during loading is represented by the evolution of dislocation density within the PSB multiplied by the cross-sectional area of the PSB: $(\rho - \rho_o)hL$. This energy contribution is dependent on the individual slip increment, ∂X_i for movement of a dislocation after nucleation.

3.2.2. Dislocation–GB Interactions to form extrusions

As previously mentioned, dislocations glide within the PSB and as a result the dislocations interact with the GB. Depending on the character of the GB, there are different energy barriers for dislocations to penetrate the GB. Once again, this value is specific to the CSL Σ value, as measured from MD simulation (Fig. 5c). The relationship between the energy barriers for a dislocation to penetrate the GB, $E_{MD}^{\gamma\text{-}slip\text{-}GB}$, and the static GB energy is given by (Appendix C):

$$E_{MD}^{\gamma\text{-}slip\text{-}GB} = 2.8 \times 10^{13} \cdot \left(E_{Static}^{GB}\right)^{-0.6} \tag{12}$$

In cases where the dislocations traverse the GB, the PSB forms a static extrusion at the GB, as shown in Fig. 4. The intersection between the PSB and GB is a preferred site for crack initiation, as pointed out by Mughrabi et al. (1983) and Weidner et al. (2006)). Thus, we must account for the formation of a static extrusion at the GB of the polycrystal; hence the associated energy with the PSB–GB interaction resulting in dislocation pile-ups and step/ledge features at the GB is given by:

$$E_{interaction}^{PSB-GB} = \sum\nolimits_i \partial X_i \cdot E_{MD}^{\gamma\text{-}slip\text{-}GB} n_{dis}^{pen} \vec{b}h \tag{13}$$

where n_{dis}^{pen} is the number of dislocations that penetrate the GB. This quantity can be approximated based on the AFM measurements of extrusions at the surface of a Ni-based superalloy by Risbet and Feaugas (2008), Risbet et al. (2003, 2009). In their study, they measured the height of the extrusions, which we normalize by the Burgers vector, $\boldsymbol{b}$, to obtain n_{dis}^{pen}. The extrusion height was measured as it evolved with increasing load cycles for various applied strain ranges. After a threshold number of loading cycles, N_{th}, the extrusions appeared and were pronounced; as expected, extrusions are observed after fewer cycles at higher applied strain ranges compared to lower strain ranges. The functional format, $G(N)$, used to fit this data is a square root dependency, based on Mughrabi and Essman's model of surface roughness (Differt et al., 1986; Essmann et al., 1981).

$$G(N) = A_2\sqrt{N - N_{th}} \tag{14}$$

Once again, the values of the AFM measurements must be normalized to account for different microstructure conditions (Appendix B).

Please cite this article in press as: Sangid, M.D., et al. The role of grain boundaries on fatigue crack initiation – An energy approach. Int. J. Plasticity (2010), doi:10.1016/j.ijplas.2010.09.009

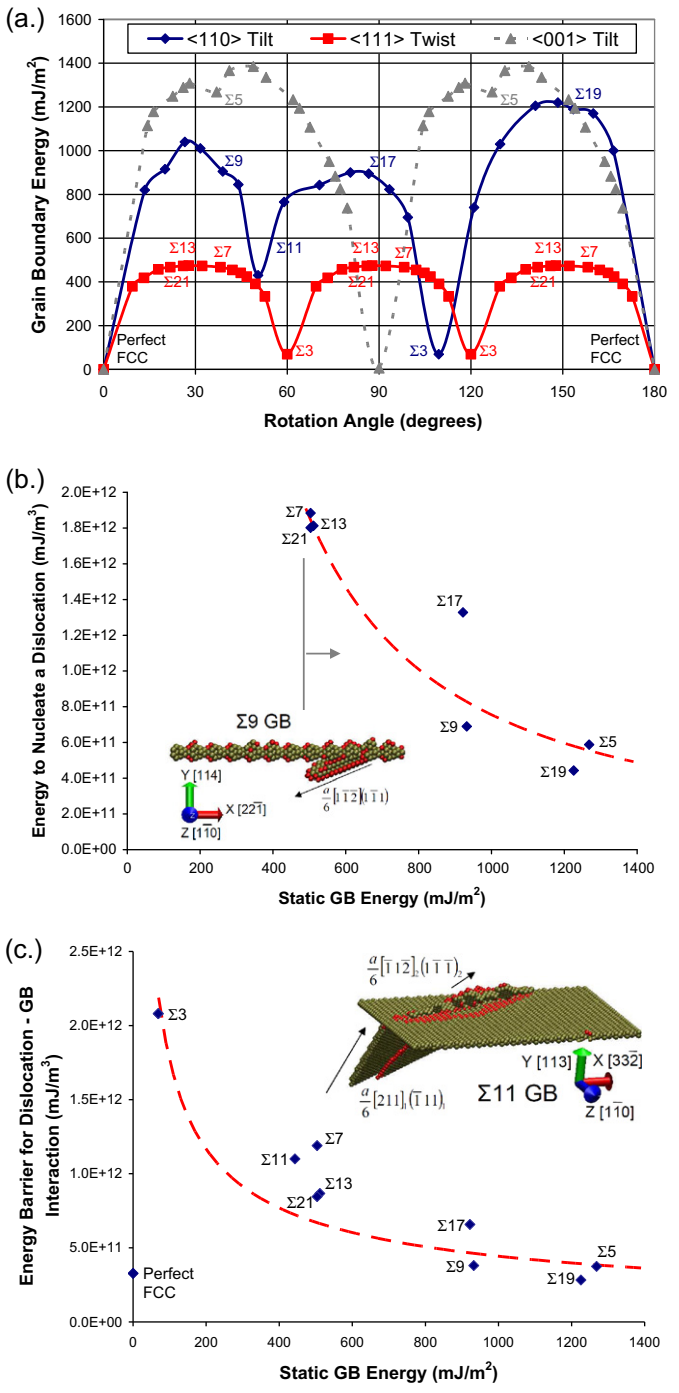

Fig. 5. (a) The grain boundary energy shown as a function of the rotation angle for nickel in the ⟨1 1 0⟩ tilt, ⟨1 1 1⟩ twist, and ⟨0 0 1⟩ tilt directions. GB characters are described in Appendix A. (b) Energy barriers for slip to nucleate from a GB plotted against the static GB energy for various types of Σ CSL value GBs. The data range is only valid to the right of the gray solid line, since dislocations did not nucleate at the GB in cases of low GB energy in the MD simulation. (c) Energy barriers for slip to penetrate a GB plotted against the static GB energy. In each plot Sangid et al. (2010), there is a relationship between the static GB energy and GB energy barrier as shown by the power law fit of the data (red dash line). (For interpretation of the references to colour in this figure legend, the reader is referred to the web version of this article.)

3.2.3. Dislocations shearing the matrix and γ' precipitates to from PSBs

Slip bands form in the material by cutting through the γ matrix and the γ' precipitates. In order to do so, the dislocation must overcome an associated energy based on the glissile partial dislocation destroying the (FCC) lattice stacking sequence

in the γ matrix and stacking sequence and order in the γ' precipitates, which correspond to the stacking fault, γ_{SF}, and anti-phase boundary, γ_{APB} (APB) energy, respectively. The γ' precipitates are composed of Ni_3Al-type in an ordered $L1_2$ structure, thus the ordering of the Ni and Al atoms within the lattice create the additional obstacle to slip. Hence, the energy associated with the formation of the PSB from shearing the γ matrix and the γ' precipitates is given by:

$$E_{APB} + E_{\gamma\text{-}SF} = \left(f \int_o^L \gamma_{APB} dL + (1-f) \int_o^L \gamma_{SF} dL \right) n_{eff}^{layers} \partial X \tag{15}$$

where f is the volume fraction of γ' precipitates and n_{eff}^{layers} is the number of effective layers contributing to the stacking fault or APB energy, as each additional layer provides 95% of the energy value of the prior layer. For U720, the fraction of γ' precipitates is approximately 0.20, which was determined by the use of image analysis software on optical micrographs.

3.3. Extension to polycrystalline material

Thus far, we have established an energy balance based on a PSB in the most favorably oriented grain of a polycrystal (Sangid et al., in press-a). This methodology can be extended to include the experimental observations of Kobayashi et al. (2009), Zhang and Wang (2000a, 2003), Zhang et al. (1998, 2003), which state that PSBs can traverse LAGBs (Fig. 6a) and are impeded by HAGBs (Fig. 6b). Hence, PSBs can form over multiple grains, as shown in Fig. 6c, which need to be accounted for in our study. From these observations, we no longer consider the most favorably oriented grain but rather the most favorable grain clusters for PSB formation and crack initiation. Many experimental and numerical analyses have addressed the role of grain–grain interaction in heterogeneous monotonic deformation (Barbe et al., 2001; Crepin et al., 2007; Efstathiou et al., 2010; Schroeter and McDowell, 2003; Zhang and Tong, 2004; Zhao et al., 2008), thus supporting our concept of grain clusters leading to fatigue damage.

From the EBSD analysis, the LAGBs are identified within the material. In these cases, the PSB is permitted to traverse the LAGB and into the adjacent grain. This can occur multiple times if LAGBs connect clusters of grains adjacent to one another, as shown in Fig. 7. In cases where a grain cluster exists, the Schmid factor of the cluster is the average of the Schmid factor of the individual grains. This is justified, since this material experiences planar slip, hence one slip system is activated in each grain and the LAGB requires a misorientation between the grains of less than 15°. Therefore, the same primary slip system is activated in the adjacent grain with only minor deviations in the slip direction. Further, the area of each grain in the cluster is summed to obtain the area of the grain cluster. The energy of the PSB traversing the LAGB, $E_{LAGB}^{\gamma\text{-}slip\text{-}GB}$, is accounted for and added to the overall energy balance (Eq. (1)) according to the following relationship:

$$E_{LAGB}^{PSB-GB} = \sum\nolimits_i \partial X_i \cdot E_{MD}^{\gamma\text{-}slip\text{-}GB} \vec{b} h \tag{16}$$

where $E_{MD}^{\gamma\text{-}slip\text{-}GB}$ is the energy barrier for slip penetration into the adjacent grain as indicated in Eq. (12).

Additionally, dislocation evolution is seen within each grain in the cluster. Hence, energy associated with dislocations nucleating and agglomerating within the PSB is taken from the most favorable GB to emit dislocations during loading.

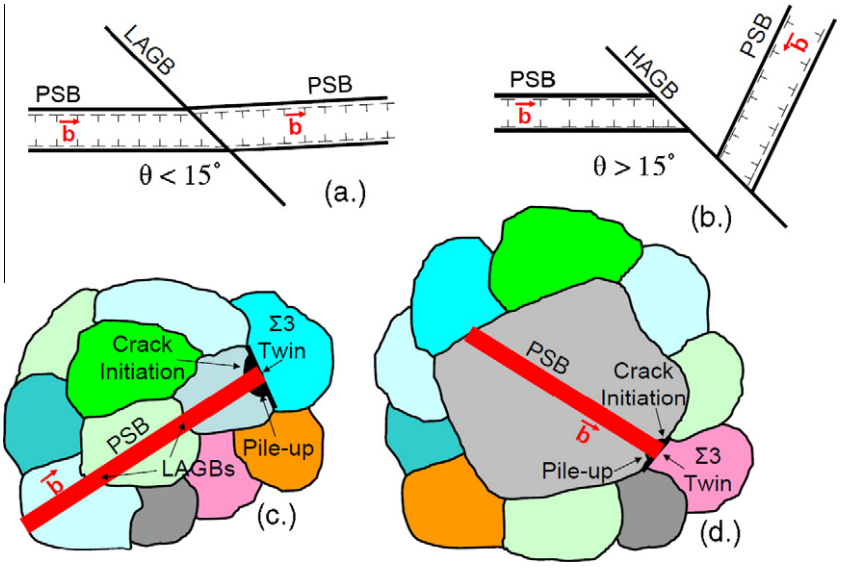

Fig. 6. (a) Transmission of a PSB through a LAGB (misorientation, $\theta < 15°$), (b) PSBs cannot penetrate through HAGBs ($\theta > 15°$). PSB are impeded by twin ($\Sigma 3$) boundaries resulting in dislocation pile-up, stress concentration, and crack initiation as shown in (c) three small grains connected by LAGBs and (d) one large grain.

Please cite this article in press as: Sangid, M.D., et al. The role of grain boundaries on fatigue crack initiation – An energy approach. Int. J. Plasticity (2010), doi:10.1016/j.ijplas.2010.09.009

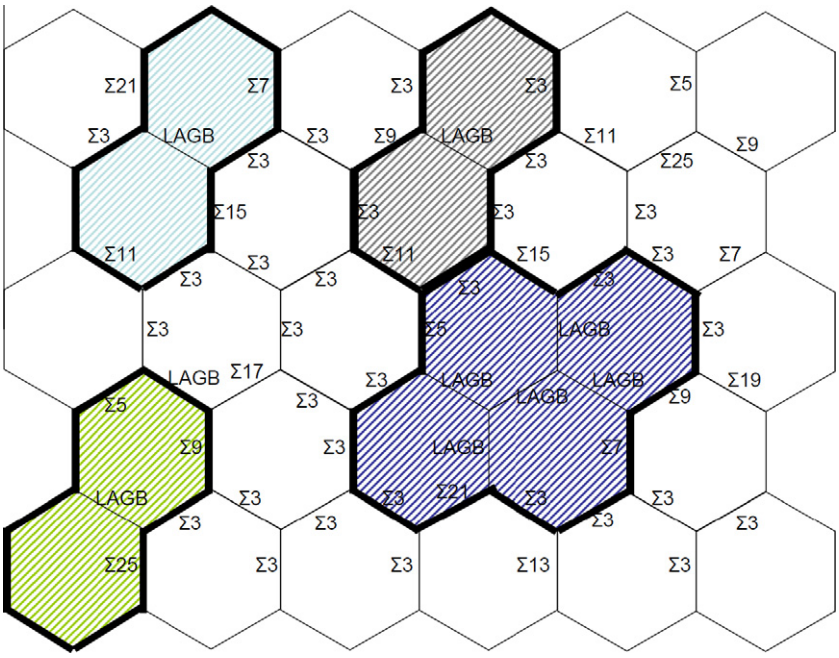

Fig. 7. Schematic of a microstructure displaying the GB characters. From experimental observation, PSBs are able to traverse LAGB. Thus, PSBs form in grain clusters connected by LAGBs as indicated. The grain sizes are shown to be uniform in this figure for the purpose of creating a simple schematic. In actuality, the grain sizes significantly vary in the EBSD scans and model. Further, the grain geometry is not specified or inherently fixed in this model; alternatively compatibility is enforced between each grain and all of its specified neighbors.

In other words, as shown in Fig. 5b, the lowest energy barrier for nucleation is analogous to the highest static GB energy, which is the GB most likely to emit dislocations within each grain of the cluster. This highest GB energy value per grain is weighted by the grain area and summed for each grain within the cluster. Hence, for a cluster containing j grains, Eq. (11) becomes:

$$E_{nuc}^{disl} = \sum_i \partial X_i \cdot \left\{ \sum_j E_{MD,j}^{\gamma\text{-}nuc\text{-}GB} L_j^2 \right\} (\rho - \rho_o) \vec{b} h \tag{17}$$

Once the chain of LAGBs is constructed, the PSB–GB interaction energy is calculated from the GB exhibiting the highest energy barrier against slip. This GB effectively impedes the PSB resulting in dislocation pile-up, static extrusions at the GB, stress concentration, and ultimately crack initiation. Therefore, the GB with the largest energy barrier analogous to the lowest static GB energy (according to Fig. 5c) is selected for the grains at the outskirts of the grain cluster; this value is used in Eq. (13) to account for PSB–GB interactions.

3.4. Failure criterion

Remaining consistent with the other historical energy balance for fracture (Griffith, 1920), twins (Cooper, 1965, 1966), dislocation emission (Rice, 1992; Rice and Thomson, 1974), and crack initiation (Tanaka and Mura, 1981), we check the stability of the PSB by differentiating with respect to plastic deformation, specifically movement of the glissile dislocations. Each component of the energy balance in Eq. (1) is expressed as an increment of slip, ∂X_i, thus making differentiation very amenable and computationally efficient. The energy evolution is updated once during each loading cycle, in doing so the results are quasi-static or rate-independent. The minimum energy of the PSB is determined:

$$\frac{\partial E}{\partial X_i} = 0 \tag{18}$$

Additionally, the second derivative of the energy must be positive to ensure that the energy corresponds to a local stable minimum. Thus, we establish Eq. (18) as our failure criterion for fatigue crack initiation corresponding to stability and equilibrium of the PSB's energy. A similar failure criterion rationale has been proposed by Huang et al. (2010) based on experimental observations, in which they suggested that dislocation self-organization may result in the formation of microcracks during fatigue loading.

Hence, this model sums the energy contributions of each term in Eq. (1) within the grain or grain cluster most likely to form a PSB (favorable energy for failure based on combination of orientation, grain size, and adjacent grain boundary character – CSL Σ values). This energy balance evolves with increasing loading cycles; meanwhile physically there is significant irreversible slip within the PSB leading to dislocations penetrating the GB thereby forming extrusions. When the PSB reaches

Please cite this article in press as: Sangid, M.D., et al. The role of grain boundaries on fatigue crack initiation – An energy approach. Int. J. Plasticity (2010), doi:10.1016/j.ijplas.2010.09.009

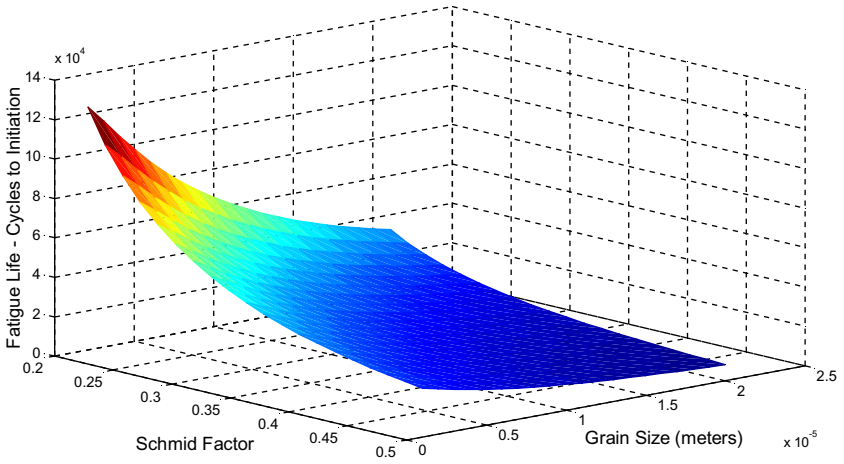

Fig. 8. Sensitivity analysis of the model based on varying the input factors for grain size, L, and Schmid factor, m. This analysis allows us to set a threshold range on grains with problematic sizes and orientations that are most likely to be the weakest link in a polycrystalline aggregate.

a minimum energy configuration, a crack initiates in an attempt to maintain low energy of the system. The crack nucleates at the site of the static extrusions (ledge and step features) at the intersection of the PSB and GB.

4. Polycrystalline fatigue model

Thus far, we have presented a methodology for predicting fatigue crack initiation based on an energy balance, which examines each grain in the polycrystalline aggregate along with the formation of clusters, i.e. grains connected by LAGBs. In a sense, a weakest link is determined and cracks initiate from the PSB–GB interaction in this grain or grain cluster. A sensitivity analysis was preformed on the fatigue model by varying the orientation and size of the grains/clusters, while the GBs character and neighboring grains are held constant. As shown in Fig. 8, the grain size (1–20 μm) and Schmid factor (0.215–0.5) were systematically varied, and the resulting fatigue lives were calculated. As expected, for large, favorably oriented grains, cracks initiated at a lower life as opposed to small grains with low Schmid factors. From this analysis, we can disregard the small grains (of size L in meters) with low Schmid factors, m, since the aggregate of grains fails from the weakest link. Hence, a threshold function is determined based on Fig. 8, whereas grains/clusters that exhibit a fatigue life of greater than 20,000 cycles were discarded. This simulated result produces the following condition based on a curve fit of Fig. 8, which must be satisfied to consider the specific grain or grain cluster in the energy balance.

$$m - 4.7x10^8L^2 + 2.6x10^4L \geqslant 0.67 \tag{19}$$

Hence, regardless of the orientation, according to Eq. (19), any grain less than 7.5 μm is not considered in the energy balance, since it is highly likely a crack will initiate elsewhere in the material. There is no upper bound to Eq. (19) as larger grains are more likely to initiate fatigue cracks. As shown in Fig. 2a, this criterion discounts approximately 80% of the grains. For example, for specimen 2 containing 3664 grains, 113 grains/clusters satisfy Eq. (19), in which 54% were single grains (Fig. 6d), 27% were grain clusters connected by a single LAGB, and 19% were grain clusters containing 3–7 grains. This simplification greatly improves computational time. Given raw EBSD data, this code locates the fatigue clusters most likely to nucleate a crack and computes the fatigue life via an energy balance for each individual grain and cluster of grains satisfying Eq. (19). Thus, cracks initiate in the specimen at the weakest link of the microstructure, from which a fatigue life is predicted. On average, for a given applied strain range, this aforementioned algorithm runs in approximately 15 s on a typical desktop computer, thus offering significant savings on computational cost versus other microstructurally driven fatigue models – such as cyclic crystal plasticity.

In order to illustrate the dominant terms in the overall energy balance (Eq. (1)), we show the energy evolution for specimens 1 and 2 at the highest and lowest applied strain ranges in Fig. 9. Each term's contribution to the energy balance along with the total energy of the PSB is shown evolving with the applied loading cycles. As discussed, the continuum terms (first three terms of Eq. (1)) provide a stress field that must be overcome for slip within the PSB. Consistent with traditional energy balances, the relaxation of the elastic stored energy (due to the external forces) appears in the energy balance (Eq. (3)), resulting in a negative value for the blue[1] line in Fig. 9. The sharp kink in the blue line for the lower strain ranges (Fig. 9b and d) occurs upon saturation of the dislocation density and the material hardening stress response to the applied external strain. The blue and light blue dashed lines represent dislocations cutting through the γ matrix and the γ' precipitates to form the PSB, which remain relatively constant throughout fatigue loading. The red dashed curve represents the energy of

[1] For interpretation of colour in Fig. 9, the reader is referred to the web version of this article.

Please cite this article in press as: Sangid, M.D., et al. The role of grain boundaries on fatigue crack initiation – An energy approach. Int. J. Plasticity (2010), doi:10.1016/j.ijplas.2010.09.009

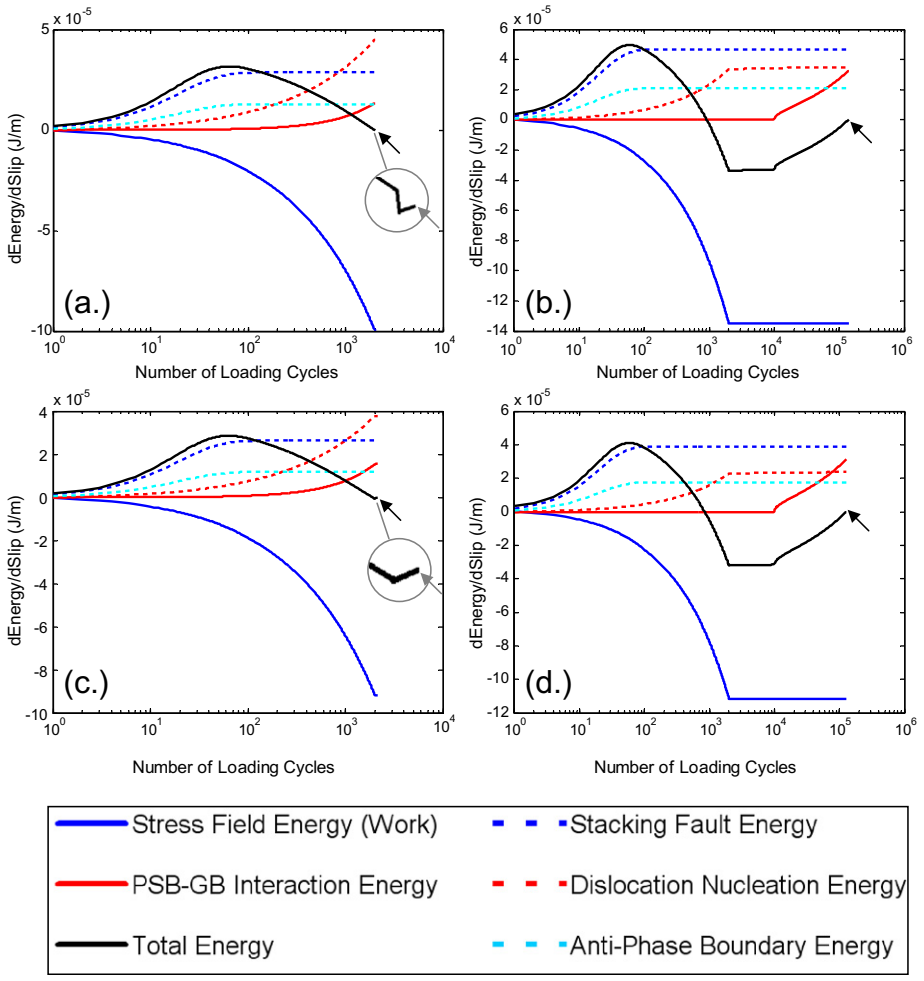

Fig. 9. The evolution of the individual and total energy components from our energy balance (Eq. (1)) with increasing loading cycles; each term is expressed as a derivate with respect to a slip increment. Hence, the total energy (black line) reaches a minimum as its derivate approaches zero, which is defined as stability of the PSB and crack initiation. Four scenarios are shown corresponding to (a) Specimen 1 at the highest applied strain range – 2009 cycles to initiation, (b) Specimen 1 at the lowest applied strain range – 140,518 cycles to initiation, (c) Specimen 2 at the highest applied strain range – 2138 cycles to initiation, and (d) Specimen 2 at the lowest applied strain range – 129,323 cycles to initiation. In Fig. 9a and c, the inset shows an enlarged image of the failure point, which indicates the total energy's derivative approaches zero with a positive slope (thus indicating a local minimum in energy).

dislocations nucleating from the GB and forming within the PSB. This value increases slightly as the dislocation density increases and saturates. Physically, cracks initiate at the static extrusions (i.e. ledges/steps) across the GB as a consequence of PSB–GB interaction, dislocation pile-up, and stress concentration; hence this corresponding energy drives the energy balance. Dislocations pile-up at the GB and eventually penetrate the GB forming extrusions, at which point the energy raises substantially as shown by the red curve. The black curve represents the total energy of the system, which is the sum of all other curves. The overall energy value is initially dominated by the applied work and later balanced by the PSB–GB interaction energy. Each of these curves represents the derivative with respect to a slip increment. Hence, as the black curve approaches zero, this corresponds to stability of the PSB and is our criterion for crack initiation. Attention must be paid to ensure that the stability refers to a minimum energy configuration of the PSB, hence the derivative of the total energy is zero and its second derivative is positive; this occurs the second time the black curve reaches zero. For clarity, this point is enlarged in the inset of Fig. 9a and c. Finally, these energy evolution plots in Fig. 9 are specific to the critical feature within the specimen's microstructure resulting in failure. Similar plots can be constructed for each GB in the aggregate, in which other terms in the energy balance have more prominent roles; hence this model is not solely driven by the PSB–GB interaction energy.

5. Discussion

Material characterization in the form of EBSD was completed on three specimens as shown in Table 1. The resulting microstructures were loaded into our fatigue model to search for grain clusters most likely to fail. From this analysis, we

determined the PSB which first nucleates a crack and the associated number of loading cycles in which this occurs. The results are shown in Fig. 10 for the theoretical fatigue life of the three simulated specimens along with the experimental log averages and log standard deviations representing 84 experiments as shown with a normalized applied strain range. It can be seen that the model results are within a single standard deviation of the experimental results, thus producing very good agreement.

The nickel-based superalloy, U720, tested in our study displays a lot of microstructure deviation (Table 1) and as a consequence, a large scatter in fatigue results is observed. The simulated specimens are no different, in the sense that specimens 1 and 2 exhibit a large standard deviation in grain size; meanwhile specimen 3 displays a very fine grain size with minimal deviation. All three specimens have a random orientation of grains, thus no texturing effects are observed. Each of the specimens has a large percentage of twins. Also, specimen 1 and 2 have more LAGBs, consequentially more grain clusters form in these two specimens.

It is expected that due to the large number of LAGBs and larger grain size, specimens 1 and 2 would have a shorter fatigue life, which is seen in the intermediate strain ranges. Although surprisingly, each of the specimen has nearly the same fatigue life over the span of the simulated strain ranges. From a statistical point of view, in the case of low cycle fatigue, which contains multiple variables, failure is not due to extreme cases (especially for instances of low applied strain ranges and large variability in the microstructure), such as unusually large grains or many connected LAGBs. Rather, the critical condition more readily occurs, due to a natural series of factors aligning themselves, such as a couple of large grains (size – one standard deviation greater then average) connected across a LAGB to form a cluster that is orientated with a high Schmid factor.

Interestingly, in Fig. 10, the fatigue life trends from the three specimens is not always the same, i.e. a given specimen type has the shortest fatigue life at a given strain range and the longest life at a different strain range. Hence, we see different terms dominate the energy balance at different strain ranges. Thus, in a given aggregate, different grain clusters are the weakest link depending on the applied strain range as shown in Table 2. At higher applied strain ranges, a cluster containing multiple grains typically fails first; meanwhile at low strain ranges, a single grain is the cause of failure. In specimen 3, the grain size is small and narrowly distributed; hence the same grain cluster fails at each strain range.

From the simulated specimens, we see the size of the clusters is in the range of 8.3–15.3 μm. This approaches the facet sizes (15–135 μm) measured from the fracture surfaces of failed fatigue experiments, as shown in Fig. 2c. We would expect to see larger grain clusters, which mimic the facet size, if more specimens are tested from EBSD scans that encompass a greater area. Another possible reason for the discrepancy between cluster size and facet size is that experimentally short cracks initiate and experience slow crack growth. These fine growth features cannot be distinguished in the facet, hence the facet is not a good measure of grain cluster size which causes crack initiation.

In each specimen, the crack initiate from a PSB–GB interaction, in which the GB is composed of a $\Sigma 3$ boundary, also known as a twin (Fig. 6c and d). Our model's results match experimental observations, (Boettner et al., 1964; Guo et al., 2005; Hashimoto et al., 1999; Llanes and Laird, 1992; Miao et al., 2009; Qu et al., 2008; Thompson, 1972), which suggest that cracks most likely initiate near a twin boundary (Fig. 3a and b). We showed that the TB has the highest energy barriers against slip (Fig. 5c). As a consequence, PSBs are impeded resulting in high stress concentration, higher energy, and crack formation. Physically, the material alleviates the high resolved shear stress by nucleating a crack.

As aforementioned, in literature the role that twins play in the fatigue response of a material is still an issue of debate. From our analysis, we establish their role as follows. Twins are both beneficial and detrimental to the fatigue performance. As shown, in Fig. 5, TBs exhibit the lowest static energy as well as the highest energy barrier for dislocation nucleation and slip transmission. Hence, twins have an important role in the macroscopic hardening of the material, since coherent symmetric twin boundaries do not allow for emission of dislocations and further confine their motion. Tschopp and McDowell

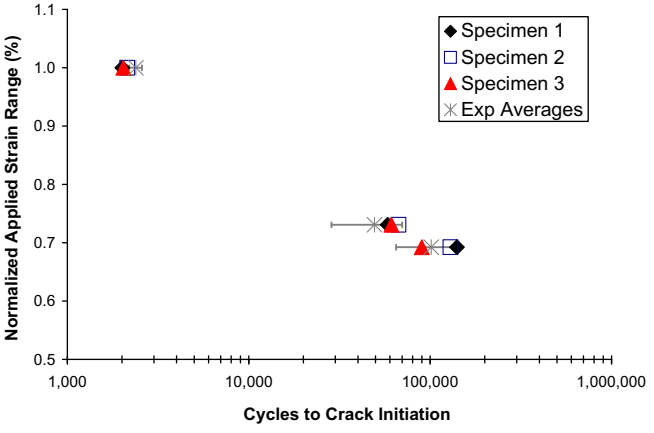

Fig. 10. Predicted fatigue results for the three specimens which were characterized by EBSD scans (Table 1). The predictions are compared to experimental log averages and log standard deviations based on 84 fatigue experiments. Please note the applied strain ranges are normalized values.

Please cite this article in press as: Sangid, M.D., et al. The role of grain boundaries on fatigue crack initiation – An energy approach. Int. J. Plasticity (2010), doi:10.1016/j.ijplas.2010.09.009

Table 2
Model predicted fatigue results in terms of number of cycles until crack initiation for three specimens at a range of normalized applied strains. The location in the microstructure, i.e. weakest link – grain or grain cluster, where the crack initiates is illustrated by the number of grains within the cluster (1 if a single grain), Schmid factor, size, and GB character in which PSB–GB interaction takes place.

Specimen number	Normalized strain range	Cycles to initiation	# of Grains within cluster	Schmid factor	Cluster size (μm)	CSL Σ value
1	1.00	2009	3	0.493	9.39	3
1	0.92	2055	1	0.460	12.94	3
1	0.85	2785	1	0.492	15.29	3
1	0.77	17,795	1	0.492	15.29	3
1	0.73	58,306	1	0.492	15.29	3
1	0.69	140,518	1	0.492	15.29	3
2	1.00	2138	3	0.493	8.63	3
2	0.92	2271	2	0.486	11.03	3
2	0.85	5876	2	0.429	12.99	3
2	0.77	23,185	1	0.483	12.80	3
2	0.73	66,913	1	0.483	12.80	3
2	0.69	129,323	1	0.483	12.80	3
3	1.00	2036	2	0.497	8.34	3
3	0.92	4437	2	0.497	8.34	3
3	0.85	10,270	2	0.497	8.34	3
3	0.77	23,864	2	0.497	8.34	3
3	0.73	61,104	2	0.497	8.34	3
3	0.69	89,847	2	0.497	8.34	3

have shown that asymmetric $\Sigma 3$ boundaries have a lower stress and associated activation energy for nucleating dislocations compared to symmetric twin boundaries (Tschopp and McDowell, 2007, 2008), but for the purpose of this model, all GBs are assumed to be symmetric in nature. This hardening response (as shown by the applied work curves in Fig. 9) acts to extend the fatigue life of the material. Although, in microstructures that have widely distributed grain sizes or contain a large percentage of LAGBs, PSBs are seen to form in large grains and/or multiply connected grains, i.e. grain clusters. As the PSB interacts with the TB, the results show that the TB's high energy barrier for slip, results in dislocation pile-ups, stress concentration, static extrusions, higher energy, and ultimately crack initiation. Thus, TBs are detrimental to and reduce the fatigue response once a PSB forms in materials with large grains or chains of connected LAGBs, as shown in Fig. 6c and d.

Finally, the proposed fatigue model is physically-based and incorporates features of the microstructure. In building the energy balance, four functionals are fit to experimental data: (a) the macroscopic hardening stress from fatigue experiments, (b) PSB width from TEM measurements, (c) the dislocation density evolving with number of cycles from literature for a similar nickel-based superalloy (Huang et al., 2008), and (d) PSB extrusion height (AFM) measured from literature (Risbet and Feaugas, 2008; Risbet et al., 2003, 2009). Hence minimal (arguably nonexistent) fitting parameters are used and further no extraneous fitting constants are used in this model. From this study, we can conclude that this model is in good agreement with the experimental data and is therefore validated.

6. Conclusions

This study represents a substantial effort in the field of physically-based fatigue modeling. The major contributions are as follows:

- A methodology was introduced to establish an energy balance for a PSB, which evolved with increasing fatigue cycles. The energy balance includes terms from the continuum scale to calculate the stress fields and the atomistic scale to account for GB and precipitate interactions. Stability of the PSB occurs at a minimum value of its energy, which was computed as the derivative of the total PSB energy with respect to plastic deformation (i.e. an increment of slip) reaching zero, corresponding to our failure criterion and crack initiation.
- This methodology is attractive since it is physically-based and inherently accounts for the microstructure of the material. The result of which produces the correct trends for predicting fatigue crack initiation based on applied strain range, grain size, grain orientation, GB character (CSL Σ value), PSB–GB interactions, volume fraction of γ' precipitates, and neighboring grain information; all of which have a significant impact on the fatigue life of the material.
- PSB are more likely to form in large grains with favorable orientations. Although, the PSBs can traverse LAGBs, thus linking grains together to form grain clusters. In doing so, we account for groups of grains, which are likely to fail and thus modify the energy balance appropriately.
- EBSD scans were completed on three specimens. From this data, grain clusters were identified and the fatigue analysis was completed on each cluster to determine the fatigue life of the weakest link in the material. The results were in good agreement with the experimental fatigue ranges of this material, thus validating our model.

Please cite this article in press as: Sangid, M.D., et al. The role of grain boundaries on fatigue crack initiation – An energy approach. Int. J. Plasticity (2010), doi:10.1016/j.ijplas.2010.09.009

- From the three specimens, we see that the grain clusters resulting in failure exhibited a range of grain sizes and contained various numbers of grains within the clusters. Hence, extreme cases (often known as large as (ALA) grains or a large number of connected LAGBs) did not constitute failure. Further, the cracks initiated near a twin boundary, corresponding with experimental observations. Thus, the PSB–GB interactions resulted in dislocation pile-up, stress concentration, an increase in energy, and crack initiation. Additionally, we see that at various applied strain ranges, different mechanisms or terms within the energy balance dominated failure, resulting in various grain clusters representing the weakest link.

Acknowledgments

Support for this work was provided by the Rolls-Royce Corporation and the National Science Foundation, DMR 08-03270.

Appendix A. CSL identification

In this appendix, we describe the characterization of GBs, in order to gain a deeper understanding of their role. A grain boundary involves two adjacent grains connected by an interface, as shown in Fig. 11a. By including the nature of the grain boundary, one can model GBs as lattice rotations of type: twist (axis of rotation is parallel to the normal of the GB, Fig. 11b), tilt (axis of rotation is perpendicular to the GB normal, Fig. 11c), or mixed. It should be expected that a certain number of the atoms in each lattice have coincidental locations from one grain to the next. This is known as a coincident site lattice, CSL. Further, special grain boundaries come as a consequence of the CSL, by taking the reciprocal of the fraction of coincidental sites; one can obtain the CSL Σ value.

From the EBSD scan, the orientation of each grain (Euler angles) in the scan and a list of the neighboring grains were obtained. From the Euler angles, (φ_1, Φ, φ_2), the rotation matrix, g, of each grain is then found by:

$$G = \begin{bmatrix} \cos\varphi_1\cos\varphi_2 - \sin\varphi_1\sin\varphi_2\cos\Phi & \sin\varphi_1\cos\varphi_2 + \cos\varphi_1\sin\varphi_2\cos\Phi & \sin\varphi_2\sin\Phi \\ -\cos\varphi_1\sin\varphi_2 - \sin\varphi_1\cos\varphi_2\cos\Phi & -\sin\varphi_1\sin\varphi_2 + \cos\varphi_1\cos\varphi_2\cos\Phi & \cos\varphi_2\sin\Phi \\ \sin\varphi_1\sin\Phi & -\cos\varphi_1\sin\Phi & \cos\Phi \end{bmatrix} \tag{A.1}$$

This allows us to calculate the misorientation rotation matrix, Δg, between each grain and its neighbor,

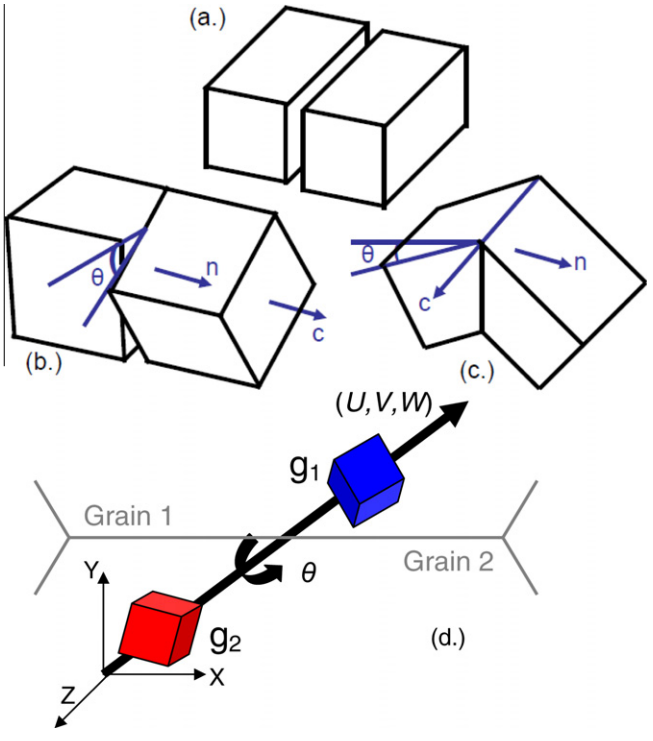

Fig. 11. (a) Schematic of two adjacent lattices, where the interface is known as a grain boundary, (b) a twist GB as the axis of rotation corresponds to the normal plane of the GB, (c) a tilt GB as the axis of rotation is perpendicular to the GB normal, and (d) schematic of the axis-angle pair for grain boundary description.

Please cite this article in press as: Sangid, M.D., et al. The role of grain boundaries on fatigue crack initiation – An energy approach. Int. J. Plasticity (2010), doi:10.1016/j.ijplas.2010.09.009

$$\Delta g = g_1^{-1} g_2 \tag{A.2}$$

However, the misorientation matrix is not unique, since FCC materials have cubic symmetry. Thus, the misorientation matrix must be rotated about threefold axes (plus the identity) or in other words multiplied by the 24 cubic symmetry operators (known as class 432, $\boldsymbol{O}_{432}$), where each symmetry operator is a rotation of the identity tensor. A loop is created over each symmetry operator to ensure that a minimum value of the misorientation between grains, Θ, is found.

$$\Theta = \min \left| \frac{\cos^{-1}\{tr(O_{432}\Delta g) - 1\}}{2} \right| \tag{A.3}$$

During the EBSD scan, the minimum misorientation to define a GB was specified as 2°, hence between two points a misorientation less than 2° was categorized as an internal grain rotation, whereas a larger misorientation indicated the presence of a GB.

We need a total of five degrees of freedom to fully characterize a GB, three for the misorientation and two to describe the plane of the GB. In this work, we utilize an axis–angle pair scheme, which specifies the misorientation across the GB with an axis of misorientation (UVW) along with an angle (θ), as shown in Fig. 11c.

$$\theta = \cos^{-1}\left(\frac{\Delta g_{11} + \Delta g_{22}\Delta g_{33} - 1}{2}\right) \tag{A.4}$$

$$(U, V, W) = \frac{(\Delta g_{23} - \Delta g_{32}, \Delta g_{31} - \Delta g_{13}, \Delta g_{12} - \Delta g_{21})}{\sqrt{(\Delta g_{23} - \Delta g_{32})^2 + (\Delta g_{31} - \Delta g_{13})^2) + (\Delta g_{12} = \Delta g_{21})^2}} \tag{A.5}$$

This gives the GB misorientation but not the GB plane. Thus, the description of the GB is matched with the axis-angle pair to specify its CSL value according to a reference table provided by Grimmer et al. that includes the axis-angle pair for 47 Σ values from $\Sigma 3$ to $\Sigma 49$ (Grimmer et al., 1974) as well as more detailed database (Olmsted et al., 2009). The allowable tolerance between the measured and reference value of axis and angle is given using the Brandon condition (Brandon, 1966):

$$\upsilon = \upsilon_o \Sigma^{-1/2}, \tag{A.6}$$

where υ_o is the misorientation limit for a low angle GB, set at 15°. Thus, a low angle GB is defined as a misorientation in the range of 2°–15° and denotes a $\Sigma 1$ GB. Further, the Brandon condition is invoked on each component of the axis–angle pair, thus $|\theta' - \theta| \leqslant \upsilon$ and $|(U', V', W') \cdot (\widehat{U}, \widehat{V}, \widehat{W})|$ must be satisfied to define a Σ GB, where the ^ and $'$ denotes the reference and measured values, respectively.

Appendix B. Justification for experimental functions

As aforementioned, four functionals are fit to experimental data and utilized in our fatigue model: (a) the macroscopic hardening stress from fatigue experiments on U720, (b) PSB width from TEM measurements of fatigued U720, (c) the dislocation density evolving with number of cycles from literature (Huang et al., 2008), and (d) PSB extrusion height (AFM) measured from literature (Risbet and Feaugas, 2008; Risbet et al., 2003, 2009). Since the two latter cases are extracted from literature for similar Ni-based superalloys and only represent one test condition, we must amend the functional form to account for more general loading and microstructure forms.

The evolution of dislocation density with loading cycles (N) was fit to a power-law equation, $F(N)$.

$$F(N) = A_1 N^{c_1} + A_2 \tag{B.1}$$

The values of the dislocation density must be normalized to account for different microstructure/loading conditions.

$$\rho \propto \frac{\left(\gamma_{ratio}^{pl}\right)^2 (m_{ratio})^2}{\exp\left(E_{ratio}^{\gamma\text{-nuc-GB}}\right)} \cdot F(N) \tag{B.2}$$

The relationship for the Schmid factor, m, and dislocation density is derived from simple expressions for the Taylor hardening and inelastic strain rate, respectively.

$$\tau = m\sigma = \alpha\mu b\sqrt{\rho} \Rightarrow \rho \propto m^2 \tag{B.3}$$

Similarly, by relating the Orowan equation to the inelastic strain rate, an expression between the dislocation density and activation energy is developed.

$$\dot{\gamma} = \vec{b}\rho\bar{v} = \dot{\gamma}_o \exp\left(\frac{-\Delta E}{kT}\right) \Rightarrow \rho \propto \exp(\Delta E) \tag{B.4}$$

Due to the volatile nature of the exponential term, a Taylor expansion was used to the second power. The plastic strain amplitude relationship was verified by experimental data by Grosskreutz (1971) for the dislocation density in copper single crystals as a function of shear flow stress, which can be related to the plastic shear strain as follows:

Please cite this article in press as: Sangid, M.D., et al. The role of grain boundaries on fatigue crack initiation – An energy approach. Int. J. Plasticity (2010), doi:10.1016/j.ijplas.2010.09.009

$$\rho \propto (\gamma^{pl})^2 \tag{B.5}$$

The extrusion height was measured as it evolved with increasing load cycles for various applied strain ranges, $G(N)$, (Eq. (14)) from AFM measurements (Risbet and Feaugas, 2008; Risbet et al., 2003, 2009). Similarly, the values of the AFM measurements must be normalized to account for different microstructure conditions. Hence the number of dislocations that penetrate the GB, n_{dis}^{pen}, to form the extrusion is proportional to the following ratios:

$$n_{dis}^{pen} \propto (\gamma_{ratio}^{pl})^2 (m_{ratio})^2 (L_{ratio}) \cdot G(N) \tag{B.6}$$

where the plastic strain ratio is confirmed by the experiments (Risbet et al., 2003) and theory (Mughrabi et al., 1983), and the grain size dependency is derived by modeling the irreversible slip in a PSB (Risbet and Feaugas, 2008). Similar arguments were made for the Schmid factor as aforementioned in Eq. (B.3) (Sangid et al., in press-a).

Appendix C. MD simulations

MD simulations were created to reconstruct CSL Σ GBs from distinct orientations of crystal lattices consisting of FCC Ni using the Foiles–Hoyt potential (Foiles and Hoyt, 2006). This EAM potential for Ni was chosen to match the intrinsic, γ_{SF}-127 mJ/m^2, and unstable, γ_{US}-255 mJ/m^2, stacking fault energies of the material, which compares well with experimental values of 125–128 mJ/m^2 and ab initio calculations of 273 mJ/m^2 (Siegel, 2005) for the γ_{SF} and γ_{US} energies, respectively. The simulation box was deformed using an NPT ensemble with periodic boundary conditions. The temperature was held constant at 10 K for these simulations, which is a necessary assumption due to the erratic stability of the simulation at elevated temperatures. The simulations have been verified at higher temperatures (300 K) and lower strain rates (108 and 109 1/s) as the resulting dislocation reactions were consistent at each of these various test parameters. The activation energy is stress-assisted, further study is needed to investigate scaling the energy barrier results with temperature and strain rate as discussed by Zhu et al. (2008). A void was introduced into the system to facilitate dislocation nucleation leading to slip-GB interaction. To grasp the role of the GBs on the energetics of each system, the potential energy of each atom was measured during the simulation. A control box was placed at the intersection of the dislocation and GB along the atoms which play a

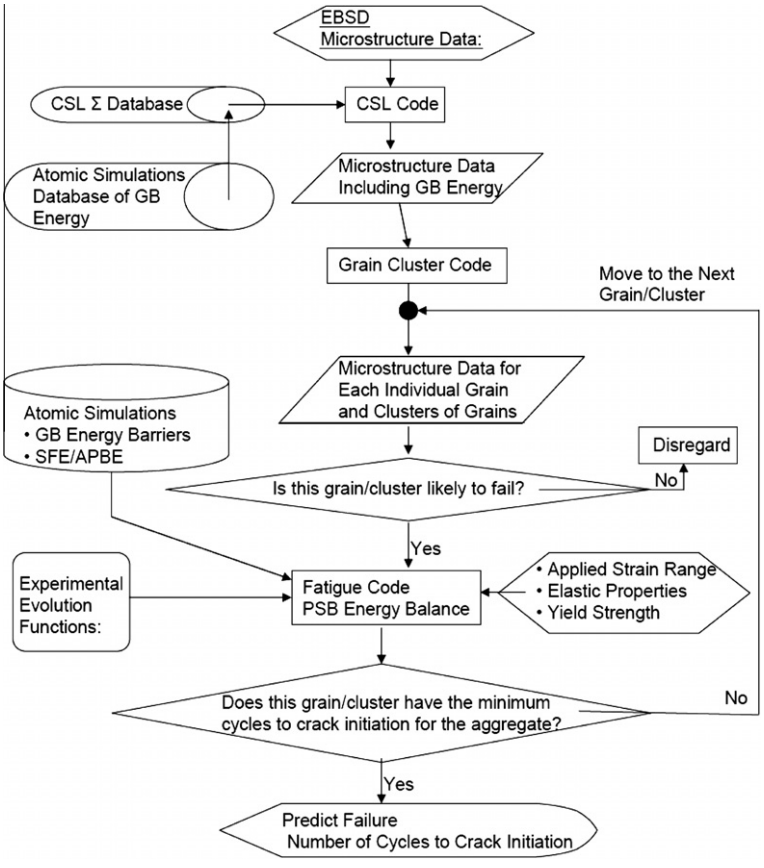

Fig. 12. Algorithm flow chart describes the microstructure-based fatigue code methodology.

Please cite this article in press as: Sangid, M.D., et al. The role of grain boundaries on fatigue crack initiation – An energy approach. Int. J. Plasticity (2010), doi:10.1016/j.ijplas.2010.09.009

role in the interaction (selected via the centro-symmetry parameter (Kelchner et al., 1998)); hence it is not a simple cubic box. Extreme care was taken to select the positions of only the relevant defect atoms to determine the energy upon loading of that atom, which was reduced by the energy of that atom in its static relaxed position and normalized by the volume of the control box. In order to verify these MD calculations for determining the energy barrier, a system was constructed without a GB to mimic slip in an FCC lattice. The result of our MD control box method was compared to the generalized stacking fault energy and produced a modest 6% difference, thus validating this procedure.

This procedure was repeated for various CSL Σ GBs, in order to measure the energy barrier for slip transmission: $\langle 110 \rangle$ tilt – $\Sigma 3, 9, 11, 17, 19$; $\langle 111 \rangle$ twist – $\Sigma 3, 7, 13, 21$; and $\langle 001 \rangle$ tilt – $\Sigma 5$. Similarly, the void was removed from our MD system and the simulation box was deformed to measure the energy barriers associated with slip nucleation from the GB. The $\Sigma 3$ and $\Sigma 11$ GBs have a stable configuration, hence nucleation from the GB was not observed in the simulation. We rationalized the energy barriers for various types of GB with their static GB energy. The results of which are shown in Fig. 5 as the energy barrier for slip nucleating from a GB and slip transmission across a GB is plotted against the static GB energy for each GB. There is an inverse relationship between the energy barrier against slip and static energy for each type of GB. A power law function was fit to the data resulting in Eqs. (10) and (12), respectively. Details concerning the methodology of these MD simulations and a discussion of the results can be found in (Sangid et al., in press-b).

In this section, we offered a simulation based approach for obtaining the energy barriers associated with slip transmission/nucleation from a GB; since this information is extremely hard to obtain experimentally and no such analytical model can be developed (considering the complexity of certain GB types). We have calculated these energy barriers for multiple cases using atomistic simulations and generalized this approach by applying a fit to the results. This methodology offers substantial progress compared to other types of models, which approximate or back-fit (from experiments) these energy barrier values without distinguishing different GB types. Hence in doing so, we can locally/spatially evaluate the energy barriers for individual GBs, which are of particular interest for fatigue crack initiation modeling.

Appendix D. Microstructure-based fatigue algorithm

The algorithm flowchart for our microstructure-based fatigue code is shown in Fig. 12. The model reads in data from an EBSD scan in the form of grain ID, Euler angles, grain area, and a list of nearest neighbors per grain. This data is manipulated by a CSL code as described in Appendix A, which characterizes the GBs according to its CSL Σ value and assigns a corresponding GB energy from MD simulations. The ensuing data is read into the grain cluster code as described in Section 3.3, which allows PSBs to transfer through LAGBs resulting in the formation of clusters, thus producing a list of grains and grain clusters. Based on the Schmid factor and size of each grain/cluster, its probability of failing is calculated by Eq. (19). For grains that are likely to fail, the PSB energy balance is computed according to Section 3. The fatigue code requires inputs regarding the applied strain range and elastic/yield properties of the material. Finally, four experimental functionals (Appendix B) and MD simulation (Appendix C) in the form of energy barriers (Eqs. (10) and (12)) and SF/APB energy results are needed for the PSB energy balance. Thus, the number of cycles to initiate a crack, N_i, is computed for a grain/cluster in the polycrystal. This process is repeated for each grain/cluster and the number of cycles to crack initiation is predicted based on the minimum value of N_i.

References

Argon, A.S., 2008. Strengthening Mechanisms in Crystal Plasticity. Oxford University Press.
Barbe, F., Forest, S., Cailletaud, G., 2001. Intergranular and intragranular behavior of polycrystalline aggregates. 2. Results. International Journal of Plasticity 17, 537.
Biermann, H., Ungar, T., Pfannenmuller, T., Hoffmann, G., Borbely, A., Mughrabi, H., 1993. Local variations of lattice parameter and long-range internal stresses during cyclic deformation of polycrystalline copper. Acta Metallurgica et Materialia 41, 2743.
Blochwitz, C., Brechbuehl, J., Tirschler, W., 1996. Analysis of activated slip systems in fatigued nickel polycrystals using the EBSD-technique in the scanning electron microscope. Materials Science & Engineering A (Structural Materials: Properties, Microstructure and Processing) A210, 42.
Blochwitz, C., Brechbuhl, J., Tirschler, W., 1995. Misorientation measurements near grain boundary cracks after fatigue tests. Strength of Materials 27, 3–13.
Blochwitz, C., Tirschler, W., 2003. Influence of texture on twin boundary cracks in fatigued austenitic stainless steel. Materials Science and Engineering A 339, 318.
Blochwitz, C., Tirschler, W., 2005. Twin boundaries as crack nucleation sites. Crystal Research and Technology 40, 32.
Boettner, R.C., McEvily, J.A.J., Liu, Y.C., 1964. On formation of fatigue cracks at twin boundaries. Philosophical Magazine 10, 95.
Brandon, D.G., 1966. The structure of high-angle grain boundaries. Acta Metallurgica 14, 1479.
Brinckmann, S., 2005. On the role of dislocations on fatigue crack initiation. Zernike Institute for Advanced Materials, University of Groningen, Netherlands.
Buque, C., 2001. Persistent slip bands in cyclically deformed nickel polycrystals. International Journal of Fatigue 23, 459.
Buque, C., Bretschneider, J., Schwab, A., Holste, C., 2001a. Dislocation structures in cyclically deformed nickel polycrystals. Materials Science and Engineering A 300, 254.
Buque, C., Bretschneider, J., Schwab, A., Holste, C., 2001b. Effect of grain size and deformation temperature on the dislocation structure in cyclically deformed polycrystalline nickel. Materials Science & Engineering A (Structural Materials: Properties, Microstructure and Processing) (321), 631.
Burmeister, H.J., Richter, R., 1997. Investigations on the origin of grain boundary cracks in fatigued f.c.c. metals. Acta Materialia 45, 709.
Christ, H.J., 1989. On the orientation of cyclic-slip-induced intergranular fatigue cracks in face-centred cubic metals. Materials Science and Engineering A A117, L25.
Cooper, R.E., 1965. The equilibrium shape of deformation twins. Acta Metallurgica 13, 46.
Cooper, R.E., 1966. The equilibrium shape of deformation twins II. Acta Metallurgica 14, 78.
Crepin, J., Heripre, E., Dexet, M., Gelebart, L., Roos, A., Bornert, M., Caldemaison, D., 2007. Coupling between experimental measurements and polycrystal finite element calculations for micromechanical study of metallic materials. International Journal of Plasticity 23, 1512.

Please cite this article in press as: Sangid, M.D., et al. The role of grain boundaries on fatigue crack initiation – An energy approach. Int. J. Plasticity (2010), doi:10.1016/j.ijplas.2010.09.009

Differt, K., Essmann, U., Mughrabi, H., 1986. A model of extrusions and intrusions in fatigued metals II. Surface roughening by random irreversible slip. Philosophical Magazine A (Physics of Condensed Matter, Defects and Mechanical Properties) 54, 237.
Dorr, G., Blochwitz, C., 1987. Microcracks in fatigued FCC polycrystals by interaction between persistent slip bands and grain boundaries. Crystal Research and Technology 22, 113.
Efstathiou, C., Sehitoglu, H., Lambros, J., 2010. Multiscale strain measurements of plastically deforming polycrystalline titanium: role of deformation heterogeneities. International Journal of Plasticity 26, 93.
Eshelby, J.D., Frank, F.C., Nabarro, F.R.N., 1951. The equilibrium of linear arrays of dislocations. Philosophical Magazine 42, 351.
Essmann, U., Gosele, U., Mughrabi, H., 1981. A model of extrusions and intrusions in fatigued metals I. Point-defect production and the growth of extrusions. Philosophical Magazine A (Physics of Condensed Matter, Defects and Mechanical Properties) 44, 405.
Essmann, U., Mughrabi, H., 1979. Annihilation of dislocations during tensile and cyclic deformation and limits of dislocation densities. Philosophical Magazine A (Physics of Condensed Matter, Defects and Mechanical Properties) 40, 731.
Foiles, S.M., Hoyt, J.J., 2006. Computation of grain boundary stiffness and mobility from boundary fluctuations. Acta Materialia 54, 3351.
Friedel, J., 1957. A discussion on work-hardening and fatigue in metals. Proceedings of the Royal Society of London, Series A (Mathematical and Physical Sciences) 242, 145.
Griffith, A.A., 1920. The phenomena of rupture and flow in solids. Royal Society of London – Philosophical Transactions 221, 163.
Grimmer, H., Bollmann, W., Warrington, D.H., 1974. Coincidence-site lattices and complete pattern-shift lattices in cubic crystals. Acta Crystallographica, Section A (Crystal Physics, Diffraction, Theoretical and General Crystallography) A30, 197.
Grosskreutz, J.C., 1971. The mechanism of metal fatigue I. Physica Status Solidi B 47, 11.
Guo, X.L., Lu, L., Li, S.X., 2005. Dislocation evolution in twins of cyclically deformed copper. Philosophical Magazine Letters 85, 613.
Hashimoto, S., Ikehata, H., Kato, A., Kato, H., Kaneko, Y., 1999. Fatigue crack nucleation at $\Sigma 3(112)$ boundary in a ferritic stainless steel. Interface Science 7, 159.
Heinz, A., Neumann, P., 1990. Crack initiation during high cycle fatigue of an austenitic steel. Acta Metallurgica et Materialia 38, 1933.
Huang, E.W., Barabash, R.I., Clausen, B., Liu, Y.-L., Kai, J.-J., Ice, G.E., Woods, K.P., Liaw, P.K., 2010. Fatigue-induced reversible/irreversible structural-transformations in a Ni-based superalloy. International Journal of Plasticity 26, 1124.
Huang, E.W., Barabash, R.I., Yandong, W., Bj, C., Li, L., Liaw, P.K., Ice, G.E., Yang, R., Hahn, C., Pike, L.M., Klarstrom, D.L., 2008. Plastic behavior of a nickel-based alloy under monotonic-tension and low-cycle-fatigue loading. International Journal of Plasticity 24, 1440.
Kelchner, C.L., Plimpton, S.J., Hamilton, J.C., 1998. Dislocation nucleation and defect structure during surface indentation. Physical Review B (Condensed Matter) 58, 11085.
Kim, W.H., Laird, C., 1978. Crack nucleation and stage I propagation in high strain fatigue II. Mechanism. Acta Metallurgica 26, 789.
Kobayashi, S., Inomata, T., Kobayashi, H., Tsurekawa, S., Watanabe, T., 2008. Effects of grain boundary- and triple junction-character on intergranular fatigue crack nucleation in polycrystalline aluminum. Journal of Materials Science 43, 3792.
Kobayashi, S., Kamata, A., Watanabe, T., 2009. Roles of grain boundary microstructure in high-cycle fatigue of electrodeposited nanocrystalline Ni–P alloy. Scripta Materialia 61, 1032.
Kronberg, M.L., Wilson, F.H., 1949. Secondary recrystallization in copper. American Institute of Mining and Metallurgical Engineers – Journal of Metals 1, 501.
Kuhlmann-Wilsdorf, D., 1989. Theory of plastic deformation: properties of low energy dislocation structures. Materials Science and Engineering A A113, 1–41.
Kuhlmann-Wilsdorf, D., Laird, C., 1977. Dislocation behavior in fatigue. Materials Science and Engineering 27, 137.
Lewis, A.C., Jordan, K.A., Geltmacher, A.B., 2008. Determination of critical microstructural features in an austenitic stainless steel using image-based finite element modeling. Metallurgical and Materials Transactions A: Physical Metallurgy and Materials Science 39 A, 1109.
Li, P., Zhang, Z.F., Li, S.X., Wang, Z.G., 2008. Comparison of dislocation patterns in cyclically deformed fcc metals. Scripta Materialia 59, 730.
Lim, L.C., 1987. Surface intergranular cracking in large strain fatigue. Acta Metallurgica 35, 1653.
Lim, L.C., Raj, R., 1985. Continuity as slip screw and mixed crystal dislocations across bicrystals of nickel at 573 K. Acta Metallurgica 33, 1577.
Lin, T.H., Ito, Y.M., 1969. Mechanics of a fatigue crack nucleation mechanism. Journal of the Mechanics and Physics of Solids 17, 511.
Lin, T.H., Wong, K.K.F., Teng, N.J., Lin, S.R., 1998. Micromechanic analysis of fatigue band crossing grain boundary. Materials Science and Engineering A A246, 169.
Liu, W., Bayerlein, M., Mughrabi, H., Day, A., Quested, P.N., 1992. Crystallographic features of intergranular crack initiation in fatigued copper polycrystals. Acta Metallurgica et Materialia 40, 1763.
Llanes, L., Laird, C., 1992. The role of annealing twin boundaries in the cyclic deformation of f.c.c. materials. Materials Science & Engineering A (Structural Materials: Properties, Microstructure and Processing) A157, 21.
Miao, J., Pollock, T.M., Wayne Jones, J., 2009. Crystallographic fatigue crack initiation in nickel-based superalloy Rene 88DT at elevated temperature. Acta Materialia 57, 5964.
Mughrabi, H., 1983. Dislocation wall and cell structures and long-range internal stresses in deformed metal crystals. Acta Metallurgica 31, 1367.
Mughrabi, H., Wang, R., Differt, K., Essmann, U., 1983. Fatigue crack initiation by cyclic slip irreversibilities in high-cycle fatigue. ASTM, Dearborn, MI, USA. p. 5.
Olmsted, D.L., Foiles, S.M., Holm, E.A., 2009. Survey of computed grain boundary properties in face-centered cubic metals: I. Grain boundary energy. Acta Materialia 57, 3694.
Peralta, P., Llanes, L., Bassani, J., Laird, C., 1994. Deformation from twin-boundary stresses and the role of texture: application to fatigue. Philosophical Magazine A (Physics of Condensed Matter, Defects and Mechanical Properties) 70, 219.
Qu, S., Zhang, P., Wu, S.D., Zang, Q.S., Zhang, Z.F., 2008. Twin boundaries: strong or weak. Scripta Materialia 59, 1131.
Rice, J.R., 1992. Dislocation nucleation from a crack tip: an analysis based on the Peierls concept. Journal of the Mechanics and Physics of Solids 40, 239.
Rice, J.R., Thomson, R., 1974. Ductile versus brittle behaviour of crystals. Philosophical Magazine 29, 73.
Risbet, M., Feaugas, X., 2008. Some comments about fatigue crack initiation in relation to cyclic slip irreversibility. Engineering Fracture Mechanics 75, 3511.
Risbet, M., Feaugas, X., Guillemer-Neel, C., Clavel, M., 2003. Use of atomic force microscopy to quantify slip irreversibility in a nickel-base superalloy. Scripta Materialia 49, 533.
Risbet, M., Feaugas, X., Guillemer-Neel, C., Clavel, M., 2009. Damage in nickel base superalloy: influence of local parameters measured by electron backscattered diffraction and atomic force microscopy. Scripta Materialia 60, 269.
Sangid, M.D., Maier, H.J., Sehitoglu, H., in press-a. A physically-based fatigue model for prediction of crack initiation from persistent slip bands in polycrystals. Acta Materialia.
Sangid, M.D., Ezaz, T., Sehitoglu, H., Robertson, I.M., in press b. Energy of slip transmission and nucleation at grain boundaries. Acta Materialia.
Sangid, M.D., Sehitoglu, H., Maier, H.J., Niendorf, T., 2010. Grain boundary characterization and energetics of superalloys. Materials Science and Engineering A 527, 7115.
Schroeter, B.M., McDowell, D.L., 2003. Measurement of deformation fields in polycrystalline OFHC copper. International Journal of Plasticity 19, 1355.
Seeger, A., Diehl, J., Mader, S., Rebstock, H., 1957. Work-hardening and work-softening of face-centred cubic metal crystals. Philosophical Magazine 2, 323.
Siegel, D.J., 2005. Generalized stacking fault energies, ductilities, and twinnabilities of Ni and selected Ni alloys. Applied Physics Letters 87, 1.
Sofronis, P., Birnbaum, H.K., 1995. Mechanics of the hydrogen–dislocation–impurity interactions I. Increasing shear modulus. Journal of the Mechanics and Physics of Solids 43, 49.
Stroh, A.N., 1957. A theory of the fracture of metals. Advances in Physics 6, 418.

Please cite this article in press as: Sangid, M.D., et al. The role of grain boundaries on fatigue crack initiation – An energy approach. Int. J. Plasticity (2010), doi:10.1016/j.ijplas.2010.09.009

Sumigawa, T., Kitamura, T., 2004. Nucleation of slip bands near twin boundary in high-cycle fatigue. JSME International Journal, Series A (Solid Mechanics and Material Engineering) 47, 98.
Tanaka, K., Mura, T., 1981. A dislocation model for fatigue crack initiation. Journal of Applied Mechanics 48, 97–103.
Thompson, A.W., 1972. The influence of grain and twin boundaries in fatigue cracking. Acta Metallurgica 20, 1085.
Tschopp, M., McDowell, D., 2007. Structural unit and faceting description of Σ3 asymmetric tilt grain boundaries. Journal of Materials Science 42, 7806.
Tschopp, M.A., McDowell, D.L., 2008. Dislocation nucleation in 3 asymmetric tilt grain boundaries. International Journal of Plasticity 24, 191.
van der Giessen, E., Needleman, A., 1995. Discrete dislocation plasticity: a simple planar model. Modelling and Simulation in Materials Science and Engineering 3, 689.
Wang, Z.G., Zhang, Z.F., Li, X.W., Jia, W.P., Li, S.X., 2001. Orientation dependence of the cyclic deformation behavior and the role of grain boundaries in fatigue damage in copper crystals. Materials Science and Engineering A 319–321, 63.
Weidner, A., Beyer, R., Blochwitz, C., Holste, C., Schwab, A., Tirschler, W., 2006. Slip activity of persistent slip bands in polycrystalline nickel. Materials Science & Engineering A (Structural Materials: Properties, Microstructure and Processing) (540), 435–436.
Zhang, N., Tong, W., 2004. An experimental study on grain deformation and interactions in an Al-0.5%Mg multicrystal. International Journal of Plasticity 20, 523.
Zhang, Z.F., Wang, Z.G., 2000a. Comparison of fatigue cracking possibility along large- and low-angle grain boundaries. Materials Science & Engineering A (Structural Materials: Properties, Microstructure and Processing) A284, 285.
Zhang, Z.F., Wang, Z.G., 2000b. Interactions of persistent slip bands with a grain boundary on the common primary slip plane in a copper bicrystal. Philosophical Magazine Letters 80, 149.
Zhang, Z.F., Wang, Z.G., 2000c. Relationship between the fatigue cracking probability and the grain-boundary category. Philosophical Magazine Letters 80, 483.
Zhang, Z.F., Wang, Z.G., 2003. Dependence of intergranular fatigue cracking on the interactions of persistent slip bands with grain boundaries. Acta Materialia 51, 347.
Zhang, Z.F., Wang, Z.G., Eckert, J., 2003. What types of grain boundaries can be passed through by persistent slip bands? Journal of Materials Research 18, 1031.
Zhang, Z.F., Wang, Z.G., Li, S.X., 1998. Fatigue cracking possibility along grain boundaries and persistent slip bands in copper bicrystals. Fatigue & Fracture of Engineering Materials & Structures 21, 1307.
Zhao, Z., Ramesh, M., Raabe, D., Cuitino, A.M., Radovitzky, R., 2008. Investigation of three-dimensional aspects of grain-scale plastic surface deformation of an aluminum oligocrystal. International Journal of Plasticity 24, 2278.
Zhu, T., Li, J., Samanta, A., Leach, A., Gall, K., 2008. Temperature and strain-rate dependence of surface dislocation nucleation. Physical Review Letters 100, 025502.

Please cite this article in press as: Sangid, M.D., et al. The role of grain boundaries on fatigue crack initiation – An energy approach. Int. J. Plasticity (2010), doi:10.1016/j.ijplas.2010.09.009